LIBRARY AWARD FOR UNDERGRADUATE RESEARCH

Second Place
Science & Engineering

UC SANTA BARBARA
Library

www.library.ucsb.edu

UNIVERSITY OF CALIFORNIA

Santa Barbara

Spatial Analysis of Rooftop PV Suitability and Solar Potential and the Estimation of Potential Annual Electricity Generation of UCSB Campus and Isla Vista:

By

Chenjia Liu

A senior thesis submitted for the degree of

Bachelor of Science

in

Environmental Studies

Thesis Advisor:

Ranjit Deshmukh, Assistant Professor, Environmental Studies

May, 2022

Abstract

Spatial Analysis of Rooftop PV Suitability and Solar Potential and the Estimation of Potential

Annual Electricity Generation of UCSB Campus and Isla Vista:

By

Chenjia Liu

Renewable energy sources are expected to play a vital role in meeting California's goal of reducing greenhouse gas emissions to 40 percent below 1990 levels by 2030. The UCSB campus and Isla Vista community have abundant solar resources and large suitable areas for rooftop PV panels and community solar projects. In this project, a spatial analysis was conducted to identify suitable areas for rooftop solar PV and calculate the solar potential. Although past studies have conducted solar potential analysis in various locations, microscale planning methods are developed in this study to more accurately reflect the solar potential. Using lidar point clouds and solar radiation data, processed in ArcGIS pro, the suitable rooftop areas for solar PV installation are identified. There are 1.31 square kilometers of areas that are suitable for solar PV installation in Isla Vista and the UCSB Campus. If all suitable areas are covered with solar panels, the potential for annual electricity generation was estimated as 208.67 GWh, which accounts for 7.55% of Santa Barbara's annual electricity consumption in 2020. Further, 94 percent of this potential was identified as being suitable for community solar projects. The findings in this study can be used as a reference for future development in order to meet the clean energy goal. This study can be extended by studying the segmentation and creating the 3D models of the building to classify the most favorable building morphology and identify the suitable classes.

Acknowledgment

This paper and the research behind it would not have been possible without the exceptional support of my supervisor, Ranjit Deshmukh. His enthusiasm, knowledge, and exacting attention to detail have been an inspiration and kept my work on track from my first encounter with the solar PV topic to the final draft of this paper. I would also like to thank my thesis class instructor, Jennifer Martin, for introducing me to this path and consistently supporting me both mentally and academically. I appreciate her unfailing patience in answering numerous questions about the language, format, and all the general ideas. I can't believe how hard it would be for me to complete this research without her help.

Dr. Michael Brown and Professor Simone Pulver have also provided thoughtful ideas about my topic. Jon Jablonski, Director of Interdisciplinary Research Collaboratory from the UCSB Library, not only walk me through the data collection process but also provide me with the most updated orthophotos and buildings of the UCSB campus.

I am also grateful for the insightful comments offered by Lynn Wu, Marian Walker, and all the peer reviewers from the Senior thesis class. The generosity and expertise of one and all have improved this study in innumerable ways and saved me from many errors.

I also want to say thank you to my dad and mom. Even though they are not with me since I started this study, their encouragement is the biggest motivation for me to move forward. Finally, I would like to thank the Environmental Studies department at UCSB for providing a valuable opportunity to conduct original research as an undergraduate.

List of Figures

List of Tables

Chapter 1: Introduction

1.1 Introduction

Since the early 1800s, the fossil fuel industry has enabled the development of technology and its dependent economies for hundreds of years. The demand for fossil fuels has not stopped increasing with the increase in our societies' populations contributing to this growth (Kannan & Vakeesan, 2016); (Sampaio & González, 2017). As a result, resources available worldwide are getting depleted, leading to severe energy crises in the 21st century (Kannan & Vakeesan, 2016).

Moreover, the exploitation of fossil fuels has caused many environmental issues such as climate change, acid rain, and air pollution (Sampaio & González, 2017). Among these issues, climate change is the primary long-term threat that the entire human race is facing. The climate change resulting from emitting carbon dioxide into the atmosphere is mostly irreversible for 1,000 years after emissions stop (Solomon et al., 2009). In order to act proactively to address the issues posed by climate change, meet carbon neutrality, and avoid an energy crisis, a shift from generating electricity from traditional fossil fuel to renewable energy, such as solar, wind, hydropower, and geothermal energy, is necessary.

Among different sources of renewable energy, solar energy represents the most promising option. Solar energy is emitted by the sun at the rate of 3.8×10^23 kW, and about 1.8×10^14 kW is intercepted by the earth in the form of heat and light (Sampaio & González, 2017). This means that solar energy has the potential to support world energy demand even though only a tiny portion of incoming irradiance is utilized to generate electricity. Some benefits of generating electricity by solar energy include a lack of atmospheric emissions or radioactive waste during use and improving long-term economic growth (Nguyen & Pearce,

2012). Moreover, the utilization of solar energy does not have to go through the process of extraction, refinement, and transportation to the generation site (Sampaio & González, 2017).

However, this isn't to say that solar energy is without limits or costs. The manufacture of solar modules with high efficiency and low cost requires cadmium telluride, and the mining of the metals can cause many other environmental issues due to the toxicity of cadmium (Sampaio & González, 2017). Large-scale utilization of commercial solar energy can also lead to land use and cover change, which can cause loss of habitat and biodiversity (Hernandez et al., 2014). Given that there is no one perfect solution, and the benefit of solar energy can outweigh the cost, solar energy plays an essential role in reducing carbon emissions. Solar energy can be harvested both at the industrial and household levels, providing more flexibility with more public involvement. Moreover, producing electricity by harvesting solar energy through photovoltaic panels (PV) is considered to be "one of the most promising markets in the field of renewable energy" (Sampaio & González, 2017). Therefore, the study of how solar energy can be efficiently used has never stopped.

In 2020, renewable energy generation accounted for 20 percent of total electricity generation in the US, with only 2.3 percent coming from solar power, and fossil fuel generation still comprising 60 percent of the share the overall energy produced (*U.S. Energy Information Administration (EIA)*, n.d.). In developing countries with less infrastructure available and relatively relaxed energy policies, the situation is worse. According to the Energy Information Administration, 63 percent of world gross electricity production came from fossil fuels in 2019, and solar only accounted for 2.6 percent. Given that generation of electricity from solar energy can reduce carbon emissions in the energy production sector and the fact that there is a great potential for increasing solar PV installation, this project will specifically focus on the amount of

solar potential that can be harvested in certain areas in California, and the factors that affect the solar potential.

1.2 Research Question

PV panels are one of the most common ways for large and small-scale solar energy utilization. Given a specific area, the efficiency of the solar PV is determined by two key factors: solar radiation distribution and its intensity (Kannan & Vakeesan, 2016). In this thesis, these two factors will be used as inputs rather than variables since they are constant throughout the target site of study, Isla Vista, and the Campus of the University of California, Santa Barbara. The potential location of solar PV panels is broad, such as the facade and rooftops of buildings. This thesis project focuses on rooftop solar PV and will try to identify any suitable site for community solar projects which is otherwise unsuitable for other uses due to area limits or location limits. This could include space between roads and fences and parking lot shade structures. According to the Office of Energy Efficiency and Renewable Energy's definition, Community solar is defined as "any solar project or purchasing program, within a geographic area, in which the benefits of a solar project flow to multiple customers such as individuals, businesses, nonprofits, and other groups"(*Community Solar Basics*, n.d.)*U.S. Department of Energy*, n.d.). Rooftop PV is analyzed individually in residential areas because there is much research about national solar rooftop potential and the geographic range is too broad for this project to cover.

Rooftop PV panels have the potential to support electricity demand for residential, commercial, and public demand in urban areas (Bazán et al., 2018). However, based on the aerial photo of the study site, the coverage of both rooftop and ground-mounted solar panels has great potential to increase. Therefore, this thesis will conduct an in-depth spatial analysis of the area potential, which includes rooftop PV potential and areas that are suitable for community solar

PV installation, and solar potential in the study site mentioned above, to help understand how solar panels could lead to a cleaner energy structure in the study site. According to the(*U.S. Department of Energy*, n.d.), "solar rooftop potential for the entire country is the number of rooftops that would be suitable for solar power, depending on size, shading, direction, and location"; for individual rooftops, it is "the amount of solar [PV] that could be installed on that rooftop, based on its size, shading, tilt, location, and construction." This project hypothesizes that the combination of individual rooftop solar panels and community-level solar panels is able to support the electricity consumption in Isla Vista.

1.3 Rationale

1.3.1 Scholarly Contribution

There has been extensive research on how to increase the efficiency of solar PV on a commercial scale, and the technology has significantly developed. The tilt direction can affect the efficiency of rooftop solar PV panels, and their suitability for different times is also well-studied. Scholars in this field have come up with different methods to measure solar potential both on a global and small scale, and each has its own set of different assumptions. However, a method that works very well in a particular place might not be applicable due to geographical location, building type, function, layout, and cultural variance (Tian & Xu, 2021). For example, the estimation of roof solar PV potential per capita in China could be significantly different from the estimation of the target site since buildings' population density and morphology are different. Specifically, the building type in urban China is typically a skyscraper with a very high population density but a relatively small area on the rooftop. However, the typical building type in the target site of Isla Vista and environment is a two-floor residential house. As a result, the

same method cannot directly be applied in California. Therefore, this project aims to examine and evaluate different methods of calculating roof solar PV potential from the previous studies and combine them into a new method suitable for the target site and California. Also, when calculating the roof solar PV potential, the available area is a critical input, but there is no immediate statistical information (Izquierdo et al., 2008). This project will measure the total roof area and extract the area available for PV installation. Both kinds of raw data can be used for other research when doing spatial analysis. The buildings will be categorized based on their size and morphology, and the method and categorization data can support future research.

1.3.2 Policy contribution

The project's outcome will generate a map of usable roofs for solar PV panels, which provides information for local agencies about the potential of increasing the share of solar energy in electricity generation. For example, suppose substantial amounts of roofs could support solar PV panels, but only a tiny portion of them did. In that case, the local government can develop incentives and subsidies to motivate people to install household-scale PV. The project will also demonstrate the most suitable roof morphology in the target site. It could serve as a reference for future building construction. For example, policies about what types of the roof the residential unit should have can be implemented to encourage more installation of the roof PV panels. Some of the residents may not be aware of the capability of the PV installation on their roofs. This paper could also help them better understand the feasibility for individual cases and thus encourage the popularization of the roof PV panels. By examining the shading effect, there could be more specific requirements about the built environment around a building to minimize the impact on solar energy utilization. Moreover, since the morphology of the structure in the study

site could be representative, the result could potentially be applied to other residential areas in California.

1.4 Thesis statement

The hypothesis of this project would be very general and simple. After the data collection and analysis through various software processes, the result generated would include: a footprint map of the study area indicating all the roof areas, a map of the study area showing all the suitable roofs for PV installation, a set of criteria designed explicitly for the study area to assess the suitability for roof PV, estimation of the incoming solar radiation, estimation of the maximum potential generation of electricity by roof PV, and the type of building that is most suitable for roof PV installation under different conditions. Also, the buildings suitable for community solar projects will be identified. Based on the common understanding and estimation of the study area, there majority (more than 50 percent) of the buildings are suitable for solar PV installation. Most of them also have the potential for community solar programs.

1.5 Method

1.5.1 Study area

The study area, including the campus of the University of California, Santa Barbara, is located on the western coast of the United States, with a population of 27,707 (*Isla Vista, CA | Data USA*, n.d.). It's a relatively small residential area of 5.7 km2. It has a Mediterranean climate characterized by dry summers and mild, wet winters. According to Figures 1 and 2, there is abundant direct normal irradiance in the study area (about 5.5-6 kWh/sq.m/day). As a result, there is a massive potential for generating electricity through solar PV.

The method of this paper is strongly based on the previous studies, which are assessed in the next section (Chapter 2: Literature review). In general, the study is divided into two parts, where the first part focuses on identifying the roof potential, and the second part focuses on the solar potential of rooftops. The first step of part one is acquiring the Light Detection and Ranging (LiDAR) data and building footprint data. These data are then processed in ArcGIS to identify and classify each roof area's tilt, azimuth, shape, and shading. The criteria are set to determine the suitability of each roof. The calculated area of a suitable roof will be ready to estimate the solar potential in part two.

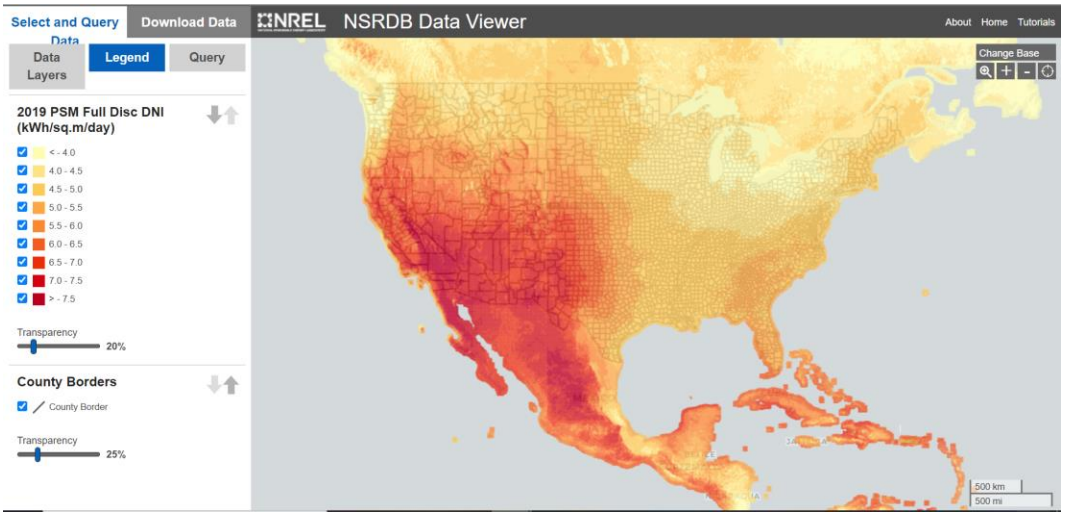

Figure 1: The direct normal irradiance of the United States. (Source: NREL)

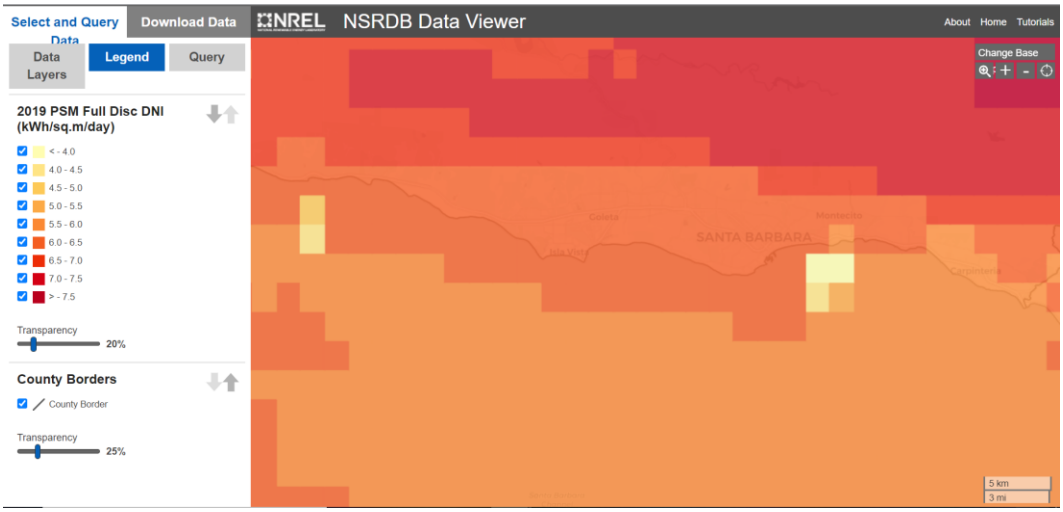

Figure 2: The direct normal irradiance of the study area. (Source: NREL)

1.5.2 LiDAR

According to the National Oceanic and Atmospheric Administration (NOAA), LiDAR is "a remote sensing method that uses light in the form of a pulsed laser to measure ranges (variable distances) to the Earth," which can provide precise information about the earth's surface. Specifically, a sensor would emit laser beams toward a target during the flight, and the laser would be reflected by the target and received by the sensor, which is shown in figure 3. The sensor precisely records the time of transmission and reflection to calculate the distance between the target and the sensor. Post-processed spatially organized LiDARdata is known as point cloud data (US Department of Commerce, n.d.). LiDAR has been used to record the Earth's surface since the beginning of the 1990s. Because of recent advances in sensor and computer technology, it has evolved into a dependable and cost-effective recording method (Quirós et al., 2018). Using ArcGIS, the mass point cloud datasets generated by LiDAR can be managed, visualized, and analyzed (US Department of Commerce, n.d.). The LiDAR data that will be used in this study is *CA SoCal Wildfires B4 2018* from the United States Geological Survey (USGS), which was collected from 2018-05-27 to 2018-10-12 and published on 2019-09-24. The USGS database

provides both Digital Elevation Model (DEM) and LiDAR point cloud in 1m resolution in LAZ. format. The completed dataset covers 3,586 km2 with 79,507,584,956 pts. However, this project will only use a small portion of the dataset covering the studied region. The density is 22.17 pts/m2.

The aerial photos of the study site are also used as a reference because when processing the LiDAR data in the ArcGIS pro, some objects with certain heights would be considered roofs by the software and can only be eliminated manually. For example, in the study of (Gergelova, Kuzevicova, et al., 2020), some buses on the street are misidentified as buildings with suitable roofs, and the authors can only know when cross-referencing the orthophotos. The UCSB Library has the most recent aerial photos and the building footprint of the UCSB campus and

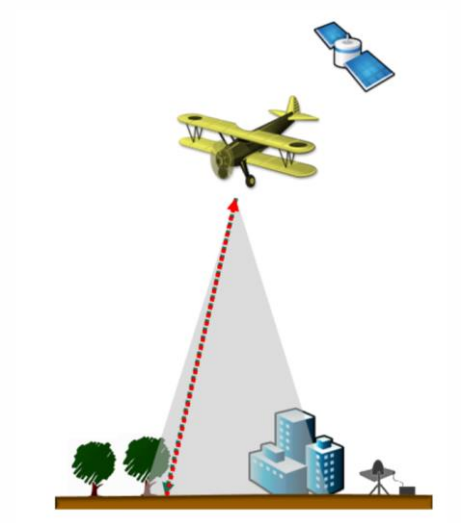

some parts of Isla vista. Both USGS and Google earth provide satellite images with high spatial resolution. However, they collected the images from many different producers, which means the specific property of the pictures is not listed. However, since this study does not utilize the orthophoto as input, the absence of property would not affect the processing and result.

Figure 3:The working principle of LiDAR.

The raw LiDAR data consists of points for the built and natural environments, such as water, vegetation, and building. In this case, only the points indicating the building would be considered valid, and any inappropriate point that does not show the roof's topography would be regarded as noise. Identifying and eliminating the noise and useless points is based on the method of (Gergelova, Kuzevicova, et al., 2020; Nguyen et al., 2012) with both a quantitative height threshold and a cross-section of the overall LiDAR points. According to (Nguyen et al., 2012), if the cut-off value is too high, some useful information will be removed; if the cut-off value is too low, near-ground points will cause distortion. Thus, a 2m lower limit will be used in this study, and the upper limit is dependent on the cross-section of the LiDAR points cloud. The points that fall onto the facade of the building are also removed. The manual identification and removal of the noise point will be made if the accuracy is not high enough.

1.5.3 Extraction and segmentation

The LiDAR points cloud is processed in ArcGIS pro to extract the roof areas and conduct segmentation. Based on the hypothesis of (Gergelova, Labant, et al., 2020) that “all roof surfaces form parts with different slopes” and “orientations and only planar roof segments can be detected, extracted, and segmented in further processing,” the buildings in the study site are categorized into six groups according to their roof planes, ridges, hips, and valleys, which are shown in figure 4. Next, to determine the edge of the roof area, a 0.3m raster size will be used to demonstrate sufficient detail based on the method of (Gergelova, Labant, et al., 2020). Generally, the segmentation can be realized by using Simplify Building and Regularize Building tools in ArcGIS based on the method of (El Merabet et al., 2015). However, in this case, the roof will be divided into the flat roof and sloped roof since they will experience different segmentation

processes. Specifically, the segmentation of the flat roof is straightforward. In contrast, the segmentation of the sloped roof requires identifying ridge-ridges, hips, and valleys of the roof to minimize the errors and capture the actual shape of the building, which can be satisfied by using the flow direction method(Gergelova, Labant, et al., 2020). According to ArcGIS(*Flow Direction (Spatial Analyst)—ArcMap | Documentation*, n.d.), the Flow Direction tool supports three flow modeling algorithms, which are mainly used in hydrology. Those are D8, Multi-Flow Direction (MFD), and D-Infinity (DINF).

Next, the extracted layer of building raster is generalized to eliminate unnecessary detail on the roof using the aggregation and regularization tools converted into polygon following the assumption that 1) "a minimum area of the roof segment; 2) preserving the squareness of the edges of objects (90°); 3) the boundary of the roof is made of a fully enclosed polygon without unnecessary holes (gaps)" (Gergelova, Labant, et al., 2020).

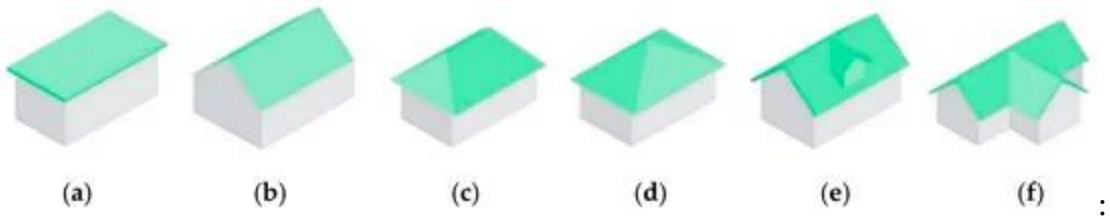

:

Figure 4:The categorization of the roof.

(a)flat—1 segment; (b) open gable—2 segments; (c) hip—4 segments; (d) pyramid hip—4 segments; (e) dormer—4 segments; (f) cross-gabled—5 segments. Source: (Gergelova, Labant, et al., 2020)

1.5.4 Slope and Azimuth

The slope is calculated using the geoprocessing tool in the 3D Analyst Tools category for every square meter of the roof. The Zonal Mean tool is used to calculate the average slope for each roof. For the purpose of simplicity, the slope of the roof will be categorized into three groups based on the method of (Gergelova, Labant, et al., 2020) : (a) 0-10 degrees; (b) 10-45 degrees; (c)45-90 degree. Any slope less than 10 degrees will be considered flat, and any slope larger than 45 degrees will be considered unsuitable. The azimuth of the roof will be categorized into 8 groups: (a) North: 337.5- 22.5 degree; (b) Northeast: 22.5-67.5 degree; (c) East: 67.5-112.5; (d) Southeast: 112.5-157.5 degree; (e) South:157.5-202.5 degree; (f) Southwest: 202.5-247.5; (g) West: 247.5-292.5 degree; (h) Northwest: 292.5-337.5 degree. The northwest, north, and northeast azimuths were defined as unsuitable. Nevertheless, any aspect value between 60 and 300 degrees will be removed to reduce the calculation time.

1.5.5 Procedure

The LiDAR data that are in LAZ. format is first converted to LAS. format in LASzip, since ArcGIS pro can only process LAS files. Then, the Classify LAS Ground tool in the Geoprocessing pane is used to identify all ground points. The ground points are necessary to generate DEM using the LAS Dataset To Raster tool, which uses a mathematical model to compute the elevation in the unknown areas based on the value of existing ground points. The value field is set as elevation. The triangulation is chosen for the interpolation type, and the natural neighbor is selected for the interpolation method. The sampling value is set as 0.5 so that it is larger than the point spacing. The rest of the parameters are left as default, and the output raster is the DEM. Next, the Classify LAS Noise tool is used to remove the unwanted points. For the method, the relative height from the ground is selected with a -2 value for minimum height.

The Classify LAS Noise tool is rerun with a different method, absolute height, to eliminate the points with abnormally high elevation. An aggressive value of 35 meters is set for maximum height because the typical height of buildings in Isla Vista is lower than this limit, and most of the noise will be removed. However, some buildings have elevations higher than 35m on the UCSB campus, and their points are also deducted. Since the buildings on the UCSB campus can be easily identified, they will be recaptured manually when creating the building footprint. After this, the Classify LAS Building tool is used to separate points that indicate the buildings from other environments. The minimum rooftop height is set as 2m, as discussed in section 1.5.2. The minimum area is set as 10 square meters.

The building footprint is ready to be extracted after pre-processing the LAS data and classification. The LAS point Statistics As Raster tool is used to create a raster of the building footprint. The most frequent class code is used for the method with a sampling value of 0.5. Although the overall shape of the buildings of the generated raster is accurate, there are some holes in the buildings, and their borders have an irregular appearance. What is more, some areas are misidentified as buildings, and some buildings are not captured. The rater is converted to a polygon using the Raster to Polygon tool to solve this problem. Note that this tool provides simple cleaning for the raster by using the Simply polygons, but it is unchecked because more sophisticated tools will be used to acquire polygons with better quality. To be specific, an expression that selects the building with an area larger than 50 (meters square) is built in the Select Layer By Attribute tool. Then, the Eliminate Polygon Part tool is used to clean the holes in the polygons. Based on observation, holes of 30 meters or less should be plugged. Then, the Regularize Building Footprint is used to clean up the jagged borders of extracted polygons. The method used is right angles, which creates buildings with clean right angles. The tolerance is set

as 1. The densification, which determines the sampling interval used to evaluate whether the regularized feature is straight or bent, is set as 1. The precision usually ranges from 0.05 to 0.25, and this project will use a value of 0.15.

After the cleaning process, most building polygons should have smooth borders with fewer holes in the polygons, while some still exist. Since there are not too many buildings in the studied site, the rest of the buildings are corrected manually using orthophoto as a reference. Specifically, the reshape and edit vertices tools are used to modify the polygons to match buildings in orthophoto. The polygons that do not fit with actual buildings will be deleted.

The next step is calculating the solar radiation. The Hillshade function is first applied to DEM, which produces a grayscale 3D representation of the terrain surface, with the sun's relative position taken into account for shading the image. This function allows the user to distinguish the buildings, trees, other surface features, and roofs, which is the project's focus. DEM is then processed with the Area Solar Radiation tool. The latitude is automatically generated based on the location, which is 34.420830. The time configuration is set as the whole year of 2022. The default value of the hour interval is once every half hour for each day. However, the parameter of once every hour will be used in the project to reduce calculation time. The calculation directions, which check the directions around each cell to find light-blocking obstacles, are given a value of 16 to reduce calculation time. Then, the building footprints will be used as a mask so that the algorithm only calculates the area with buildings. This can also reduce the calculation time. The generated solar radiation is in watt-hours per square. To make the value user-friendly, the solar radiation is converted to kilowatt-hours per square meter(kWh/m2) in the raster calculator by dividing the original value by 1000.

A layer of slope and aspect is necessary to identify the suitable rooftops. The slope layer will be created using the Surface Parameters tool based on DEM. The resulting layer will show the slope of each cell, ranging from 0 to 90 degrees. However, the areas with high slopes might not be suitable for PV installation, which will be removed using the Con tool. Based on the previous studies and the building condition in the study area, 45 degrees will be set as a cut-off value. An expression is built where a cell with a value less than or equal to 45 will be considered true. The input for false raters will be left blank to have no data value on the map. Another low slope raster will be created to only show roofs with slopes less than or equal to 10 degrees, defined as flat. The areas with incoming solar radiation less than 800kWh/m2 would be considered low. An expression to remove the areas with low radiation will also be built. The aspect layer will also be created using the Surface Parameters tool. Then, the areas that face north will be removed by building two expressions eliminating rasters with a value between 60 and 300. At this point, the raster showing areas with high solar radiation will be imported as a true raster, and the raster showing the flat roof will be imported as a false raster. As a result, the cells facing north will be replaced by values from the low slope layer, and the output layer will contain both areas that do not face north and areas with a low slope.

The power per building will also be calculated in this project using the Zonal Statistic as Table tool. This tool will look within each building's footprint polygon and aggregate the suitable cells it contains. The Building_ID will be set as a Zone field so that every building will be taken into calculation since each has a unique ID. The input value raster is set as Suitbal_Cells. The Mean is chosen for Statistics Type to determine the average solar radiation per square meter for each building. The result will be displayed as a table. However, this table will not be connected

to the spatial data on the map. The Join Field tool will be used to connect AREA and MEAN, which is the average solar radiation, to the map based on Building_Footprints.

The buildings with less than 30 square meters of suitable roof surface will also be considered unsuitable for solar panel installation. Thus, an expression where AREA is greater than or equal to 30 is built in the Select By Attributes window. The selected buildings will be exported into a new feature class using the Export Features function in the Contents pane. The usable solar radiation will be calculated and displayed in the attribute table by adding a new field in the attribute table. The data type will be set as double. Under the number format, select the numeric and round to two decimal places. Then, the usable solar radiation equals MEAN times AREA and is divided by 1000, expressed in megawatts-hour. Another field that represents electricity production is calculated. The data type and number format will be the same as the usable solar radiation. According to the best estimation of the US EPA, the solar panels are capable of converting 15 percent of incoming solar energy into electricity with a 86 percent performance ratio. Thus, electricity production is calculated by multiplying the usable solar radiation by 0.15 and 0.86 (US EPA, 2015).

1.5.6 Implication

The method used in this project will summarize and generate a set of criteria for determining the suitability of rooftop PV installation and demonstrate the suitability of each building type. The analysis can show the existing amount of rooftop solar PV versus the potential space installed with rooftop PV in the future. It could also be applied to other high-density communities with various building types on a relatively small scale, especially along the west coast of southern California. The result of the analysis could be utilized by decision-makers and potentially incorporated into the city's general plan. However, it is also important to remember

that the calculation strongly relied on assumptions and estimation based on the average data, which should be typical in general but might not be accurate enough in some individual cases.

1.6 Thesis roadmap

The rest of the paper assesses the method from previous studies and analyzes the data following the step mentioned in the method section. Chapter two reviews the methods of calculating roof potential and solar potential of earlier studies that are done in different geographic conditions. The usable assumption and criteria will be incorporated into the method of this paper. Chapter three discusses the background of solar technology and the classification and debate on community solar. Chapter 4 demonstrates the steps of data processing. The results are shown in figures and tables with an explanation and interpretation of the data. Chapter six briefly summarize the thesis project and major findings, and the limits and possible topics for future research are also discussed.

Chapter 2: Literature Review

2.1 Introduction

Generally, three methods are commonly used in the field to calculate the area of the rooftop suitable for solar PV installation (Melius et al., 2013). The first kind is constant-value methods, which uses many rule-of-thumb assumptions, such as "proportion of sloped versus flat roofs, the number of buildings with desirable rooftop orientations, the amount of space obstructed by building components (i.e., heating and ventilation), and shadows," to estimate the availability of rooftop areas (Melius et al., 2013). This kind of method is widely used, especially as a starting point for area calculation, because it requires less time and resource input and can be easily applied to large regions compared with other kinds of methods (Melius et al., 2013).

However, the tradeoff is that the uniqueness of individual buildings is not captured, which results in little validation (Melius et al., 2013).

The second kind is manual selection methods. The manual selection methods use satellite or aerial photography, Google Earth. The National Renewable Energy Laboratory's PVWatts manually identify the rooftop's suitable area, which can generate much more accurate results than constant-value methods (Margolis et al., 2017; Melius et al., 2013). Each building in the studied region will be evaluated. As a result, this method is highly time-consuming and could be impractical for extensive region analysis.

The third kind is GIS-based methods. For GIS-based methods, instead of using predetermined constant values or manually selecting buildings, the suitability is determined by GIS software after each characteristic value of what makes a suitable rooftop is fed to a computer model (Melius et al., 2013). What's more, the 3-D model generated from orthophotography or LiDAR data is the major tool to analyze the effect of solar resources and shadow (Melius et al., 2013). GIS-based methods are exceptionally efficient when calculating total solar energy generation potential because it takes slope, orientation, and building structure data into consideration (Melius et al., 2013). The GIS-based methods are more precise than constant-value and manual selection methods. They can be applied to larger spaces than the manual selection method(Margolis et al., 2017). Given the advantages of objectivity, high accuracy, and high resolution of the LiDAR data due to technological development, the GIS-based methods have become the most popular method to estimate the rooftop suitability for PV (Melius et al., 2013). In this project, the GIS-based method is most suitable for the calculation in the study site. The constant-value method is excluded because using it in a complex built environment would cause great inaccuracy. The manual selection method could be applied to the study site due to the small

scale and high accuracy, but it does not provide a systematic and efficient method that could be used in other places. As a result, the GIS-based method is the best to find a balance between accuracy and efficiency. Moreover, GIS gives both 2D and 3D views of the study site, which makes the demonstration of the building more accessible. Thus, the literature review will mainly focus on the utilization of GIS.

2.2 Method from previous studies

2.1 Calculation of solar potential

The calculation of the roof potential is necessary before calculating the solar potential. Generally, the analysis of the roof potential requires multiple steps. The first step is gathering data that could be processed in the software, such as aerial photos, LiDAR data, and building footprints. Then, the input data will be filtered and processed, such as the clean of outlier, extraction, and segmentation, in the software that is ready for calculation. However, given the frame of calculating roof potential, different authors' specific procedures and criteria could be very different. This section carefully examines the methods from previous studies to see how they could be incorporated into this project.

In *Quantification of Available Solar Irradiation on Rooftops Using Orthophotograph and LiDAR Data,* the (Yimprayoon & Navvab, 2010) use jargon-free language to introduce the general procedure of using Lidar, orthophotos, and ArcGIS to calculate the rooftop solar irradiance in a given area. The study site is in a neighborhood in Toledo, Ohio, where the Lidar data of this site is from the Center for LiDAR Information Coordination and Knowledge (CLICK) (Yimprayoon & Navvab, 2010). The data is processed in ArcGIS 9.3.1 to generate a Digital Surface Model (DSM) and a Digital Terrain Model (DTM), and these two models are

used for producing a Digital Elevation Model (DEM) by subtracting DTM from the DSM. Specifically, the DSM is generated using ground return points, and the DTM is generated using first return points. Then, the DEM is overlapped with an orthophoto of the target site so that the height of obstruction that can cause shade can be measured on every pixel. The in-situ measurements are used as a reference to understand the model's accuracy. The author claims that the measurements for trees are accurate except for deciduous trees during the leaf-off period (Yimprayoon & Navvab, 2010). After this, the 3-D models of the building and the environment of the studied site are made in Google Sketchup by importing the orthophoto from google earth according to their location in reality, and the height information is from the raster model generated by ArcGIS using lidar data. The Hillshade function in ArcGIS provides an annual duration of shade for each building. The final step is using software like Ecotect or EnergyPlus to calculate the solar potential.

This paper provides fundamental information about using LiDAR points clouds to create DEM (Digital Elevation Model) for calculating the solar irradiance on the roof. Even though this paper doesn't explicitly calculate the roof potential, the rooftop solar irradiance is a factor that affects the suitability of the roof, and the calculation of irradiance is an inevitable process for estimating the solar potential. Published in 2010, it provides basic procedures from gathering data to processing data and eventually conducting the calculation, which many later studies have followed, such as the generation of DEM and 3D models. This paper also has recognized the implication of the shading effect, but factors other than the shade are not discussed, and the criteria for suitable rooftops are not specified and considered. Still, the basic structure and flow of the analysis in this paper offer strong implications for my project, and this paper could be very

useful for modeling the Isla Vista based on the lidar data complementary to other data such as tilt and azimuth.

Two years later after the publication of the work of (Yimprayoon & Navvab, 2010), a similar method was used in (Nguyen et al., 2012)'s work with substantially more detail. In "*The Application of LiDAR to Assessment of Rooftop Solar Photovoltaic Deployment Potential in a Municipal District Unit*" (Nguyen et al., 2012) provides sufficient information on using LiDAR to conduct rapid and efficient calculation of rooftop solar PV potential on a municipal scale. Five assumptions[1] are made to apply the method to large areas and in many situations with the loss of some extent of exactness. The data used in this method include the tiled Digital Surface Model (DSM), tiled aerial photos, tiled LiDAR point clouds, and the building footprint shapefile of the target site, which are also used by (Yimprayoon & Navvab, 2010). For the LiDAR point clouds, the authors recognize that some points could have centimeter to decimeter—level horizontal errors, which might have an inaccuracy of position relative to the ground level height or other objects at a lower elevation. Thus, the elimination and buffering of those points are necessary. Four distances, ±1 m, and ±0.5 m are selected, where the positive value represents an external buffer and a negative value means that the point is lying inside the building polygon. Then, a threshold of height relative to the ground is applied to the point within the roof polygon to ensure that only the points showing the roof's profile are kept. The cut-off value needs to be carefully examined. Otherwise, the useful information might be eliminated, or the redundant information could be included. After referring to the zoning bylaw of the target city, the authors decide to use

[1] (i) individual building roof areas can be modeled properly by a composition of planer faces; (ii) anything below a chosen elevation cutoff is irrelevant for solar PV potential assessment; (iii) tree canopies are opaque; (iv) small windows on the roofs, overhangs on the walls, Heating, Vent and Air Conditioning facilities (HVACs) and antennas do not occupy so large a space that its omission adds significant area to the roof area free for PV panels; (v) the height of the object and subsequently the altimetry of the Digital Surface Model (DSM) is the difference between LiDAR's z values and an available DEM and (vi) there is no discrepancy in the form of urban structures between aerial photos (AP) and LiDAR

2.5m. The noise of anything that causes misinformation about the roof height, such as trees and chimneys, is removed by identifying the roof using maximum, minimum, and average elevations of the points within the polygon of the roof. The author claims that any point falling out of one standard deviation away from the mean elevation of the point cloud would be considered an anomalous signal. Without the outlier and noise points, the useful points are matched to corresponding aerial photos because no ArcGIS information for the building of the target city can be obtained. At this point, all the points are available to reconstruct the plane and 3D models using Random Sample Consensus (RANSAC), Singular Value Decomposition (SVD), and Triangulated Irregular Network (TIN).

Understanding the work of (Nguyen et al., 2012) is important because even though the scale of the analysis is slightly different, his study focuses on municipal levels that have high building density, which is similar to the environment in the study site. Moreover, recognizing outliers' impact and the method of assessing suitable criteria for eliminating the outliers provides implications for this project. Although the method is also based on the work of (Haala et al., 1998) and (Carneiro et al., 2009), none of these two articles is specifically related to the roof potential. Thus, the method of processing the LiDAR data in this project will be partially based on the method of (Nguyen et al., 2012). It is also important to realize that since both (Nguyen et al., 2012) and (Yimprayoon & Navvab, 2010) rely on 3D models to estimate solar irradiance, it could be the primary method for doing that. However, based on the small scale of the study site and limited time, the application of 3D modeling is not practical and beyond the scope of this paper and hence is not considered.

While the previously discussed articles focus on data processing, the criteria for determining the suitability of the roof are also required. To fully understand the method of

calculating the roof potential on different scales and the difference among them, the work of (Margolis et al., 2017), *Using GIS-based methods and lidar data to estimate rooftop solar technical potential in US cities* is also assessed. (Margolis et al., 2017) use LiDAR data and building footprint data sets to identify the total area of the rooftop and then analyze shading, tilt, and the azimuth of each rooftop at a horizontal resolution of 1 m^2 at a national level. To be specific, *the US Department of Homeland Security* (DHS) Homeland Security Infrastructure Program for 2006–2014 offers lidar data in raster format, which is produced by the first reflective surface return of lidar data and corresponding polygon shapefile of building footprints(Margolis et al., 2017). Based on the published date of this paper, the data is recent enough. Since the analysis is conducted on a national scale, the buildings are categorized into three types:

Small: < 5000 ft^2; Medium: 5000–25 000 ft^2; Large: > 25 000 ft^2(Margolis et al., 2017).

Using the standard ArcGIS Hillshade tool, the shade throughout the day is simulated (Margolis et al., 2017). The seasonal variance is demonstrated by importing data from 4 representative days: March 21, June 21, September 21, and December 21(Margolis et al., 2017). Specifically, a threshold of illumination is set to determine if a cell is in sunlight: 60% illumination for March, 70% for June, 60% for September, and 50% for December(Margolis et al., 2017). Then, the average number of hours of daily sunlight for each square meter is calculated by averaging the hours of sunlight each square meter received for four days(Margolis et al., 2017).

After that, the tilt and azimuth of each square meter of roof area are also measured and categorized. Using the tilt raster, the roof plane's mean tilt is calculated in the ArcGIS Zonal Mean tool. The roof is regarded as flat if the tilt is less than 9.5 degrees, and the tilt would be considered unsuitable if more than 60 degrees. The predicted illumination of all flat roofs needs

to multiply by 1.5 because the shading simulation underestimates the duration of sun exposure for the flat roof. The azimuth of each square meter is then categorized into one of nine azimuth classes by dividing 360 degrees into eight groups plus the group of the flat. For example, the north direction ranges from 337.5 degrees to 22.5 degrees. Note that northwest, north, and northeast (292.5–67.5 degrees) are not suitable for solar PV panels(Margolis et al., 2017). Then, the author states, "the azimuth file was then run through a variety function, which returned the number of different values in the three × three neighborhood surrounding each square meter of roof area" and assumes that "contiguous areas of identical azimuth class are a unique plane" (Margolis et al., 2017). However, specific functions were not provided. Given the tilt and azimuth of the individual planes, they are categorized into 21 orientation classes based on different combinations of tilt and azimuth.

Next, the criteria for suitability are set by the author to calculate the area of available rooftops. If the orientation is the same, how many hours in sunlight are required by a rooftop to generate 80% of the energy produced under the unshaded condition is calculated in the System Advisor Model (SAM). The requirements for azimuth and tilt are mentioned in the last paragraph. Assuming a 1.6 kW system with a 16%-efficient panel (median module efficiency from approximately 48000 systems installed during 2014) is a practical threshold based on historical data, the author states that at least 10 square meters are required for installation(Margolis et al., 2017).

Although the study scale of the work of (Margolis et al., 2017) is different from this project, the categorization of the factors that could affect the roof potential, such as azimuth, roof area, and tilt, and the criteria for determining the suitability is helpful for this project to identify the most suitable type of the building at the end. Moreover, the illumination threshold used for

accounting for the seasonal variance is also significant since the duration of the shade could be different in different seasons. Note that both (Margolis et al., 2017) and (Yimprayoon & Navvab, 2010) use the Hillshade function in ArcGIS to calculate the shading and take the sun's relative position into account.

In order to develop methods and criteria for appropriate scales that could be used in the study site, a case study of Komárno, Slovakia, is also evaluated. In *Roof's Potential and Suitability for PV Systems Based on LiDAR: A Case Study of Komárno, Slovakia*, (Gergelova, Kuzevicova, et al., 2020) use both GIS and Computer-Aided Design (CAD) software to create detailed 3D models of buildings to evaluate the roof PV potential and suitability. As mentioned above, this paper will not consider the generation of 3D models. In the first step, which is data collection and processing, the LiDAR data associated with orthophotos are used to identify the building, and it is supplemented by data from the real estate cadastre (REC) to show the building footprints registered in it. The points cloud from the LiDAR data is used for making the raster map, and the roof is highlighted by using segmentation to identify individual roof planes based on the method of (Gergelova, Labant, et al., 2020). According to the authors, segmentation plays a vital role in capturing the roof boundary and small objects. They use an independent article, *Identification of Roof Surfaces from LiDAR Cloud Points by GIS Tools: A Case Study of Lučenec, Slovakia*, to discuss "segmentation and extraction of roof objects in residential areas in the geographic information system (GIS) environment"(Gergelova, Labant, et al., 2020). The authors briefly introduce the different methods for segmentation from the previous studies, which is" a technique used to divide a surface into several non-overlapping parts" that can be used in many fields such as watersheds (Gergelova, Labant, et al., 2020). Segmentation is essential for processing input data to calculate the roof potential. The input data includes LiDAR

point cloud (*.las), photogrammetric images(*.tiff), the building footprints from the Basic Database for the GIS(ZBGIS), and the real estate cadastre. While the LiDAR points cloud and the photogrammetric images are used to identify the roof, the existing city map is used to check the absence of any building in case the data is outdated. The LiDAR point density is 19points/m2 since the recommended density for built-up areas(Gergelova, Labant, et al., 2020) with vegetation is 12-20 points/m2. The authors use a spatial filter on the cross-section of the LiDAR point clouds instead of the numerative threshold to determine whether a point is a noise. The outliers that are not located within the roof are also removed, but the procedure of this step is not given. The cleaned LiDAR point is then overlapped with the orthophoto to eliminate inaccuracy and misidentification. After all roof areas are identified, the raster with a cell size of 0.3 m(the authors have run different sizes, and the 0.3 m is their final choice) is built based on LiDAR data to show the course of the roof edges. The segmentation of the roof can be done in ArcGIS pro, which is different for flat and pitched roofs. The slope of the roof is classified into seven categories by using geoprocessing tools in the 3D Analyst Tools category in ArcGIS, where generally sloping roofs with a roof pitch of $10° < \alpha < 45°$ and flat roofs with an angle of $\alpha \leq 10°$. Using the Flow direction method, which "ensured the detection/identification of the ridge-ridges, hips, and valleys of the roof from the grid," is necessary for pitched roofs, whereas the segmentation for flat roofs is relatively simple because the roof ridge can be ignored(Gergelova, Labant, et al., 2020). The raster is then converted into a vector format for further aggregation and generalization using the Simplify Building and Regularize Building tool in ArcGIS. The authors have recognized that the relatively low point cloud density might not be able to capture the small object on the edge of the building which can affect the accuracy of measurement, while a higher density of point is recommended when it is appropriate.

Then, the spatial slope analysis based on the method (Adeleke & Smit, 2020) is used to produce a raster file DSM to extract the roof elements that might obstruct PV installation. The spatial data is processed in GIS (a combination of ArcMap 10.7.1 and ArcGIS Pro 2.4.3) and the Bentley Descartes V8i SS10 environment. The building type and the percentage of each type are identified as well. Then, the criteria for suitability are identified. Based on the previous studies, the authors state that the installation of 1 kW equipment on a roof with a minimum area of 8 m^2 is the threshold. The orientation of the roof is divided into four groups: 1—north: 315–0°, 0–45°; 2—east: 45–135°; 3—west: 135–225°; 4—south: 225–315°. Based on the result of spatial slope analysis, they are divided into three groups: flat roofs (0–10°), pitched roofs (10–60°), and very steep roofs (60–90°). The north orientation and any slope larger than 60 degrees would be considered unsuitable for solar PV. Given the suitability map, the ArcGIS Pro Solar Radiation Toolset is used for estimating the solar irradiance in 4 seasons under the ideal condition: Spring season—21 March 2020–21 June 2020; summer season—21 June 2020–23 September 2020; autumn season—23 September 2020–21 December 2020; and winter season—21 December 2020–21 March 2021. Local climatological stations collect the mean monthly sum of sunshine duration to incident solar radiation. The roof areas are divided into four groups based on the location: border(eaves, gable edge/shield edge, roof ridge), edge(ridge, saddle ridge, corner, groove, notch, degree), penetration(chimney, window, dormer), and connection(wall) when generating 3-D models, which will not be included in this paper. The weight of panels is also considered a factor since the effect of wind and snow would increase the load of the roof, which can cause an unstable structure. However, the authors did not provide any quantitative criteria for panel weight.

In recently published papers, (Gergelova, Kuzevicova, et al., 2020) and his colleague's work provides a very insightful method for estimating the suitable roof area and the solar irradiance accompanied by the previous study. They are significant for developing methods for the study site of this project since they provide a detailed procedure for capturing the real shape of the roof, and many numerical standards are offered, such as a roster size of 0.3m and the suggested points cloud density. Moreover, it provides a similar categorization of tilt and azimuth of the roof with slightly different values from the work of (Margolis et al., 2017), and both methods consider seasonal variance. This could be the result of different study scales. Because of the similar study scale and the most updated information in the work of (Gergelova, Labant, et al., 2020), the method of this project will be developed based on it.

2.2 Calculation of solar radiation

The *Solar potential of rooftops in Cáceres city, Spain,* could serve as a good reference since the studied city, *Cáceres,* is a small city of 36km^2 and has a population of 100000 (Quirós et al., 2018). It has the same Mediterranean climate as the studied area in this paper. GIS is also involved in the method of calculating solar radiation. Note that solar radiation from the last article mentioned in this section used existing data. However, it is calculated based on direct, diffuse, and reflected radiation components using methods proposed by (Hetrick et al., 1993) and incorporates the transitivity in the Spanish case study. According to (Hetrick et al., 1993), the total instantaneous insolation is the sum of the direct, diffuse, and reflected radiation components, which can be calculated using:

$$I = S_0 \tau^m \cos i + S_0 (0.271\text{-}0.706\tau^m) \cos^2 \frac{\theta}{2} \sin a + r S_0 \sin a (0.271\text{-}0.706\tau^m) \sin^2 \frac{\theta}{2}$$

where S_0 is the solar constant, τ is atmospheric transmittance coefficient, m is air mass ratio, i is the angle of incidence between the normal to the surface and the solar rays, θ is the surface slope, a is the solar elevation angle, and r is the reflected radiation coefficient.

Based on this method, the (Quirós et al., 2018) calculate transmissivity, which is "the ratio of the energy reaching the Earth's surface to that which is received at the upper limit of the atmosphere," given the direct, diffuse, and global radiation using:

$$T=GR/ER$$

Where T is the transmissivity, GR is the global radiation, and ER is the extraterrestrial radiation. ER is calculated using:

$$ER = \frac{24 \times 3600 G_{SC}}{\pi} \left(1 + 0.33 \cos \frac{360n}{365}\right) \times \left(\cos LAT \cos DEC \sin \omega_s + \frac{\pi \omega_s}{180} \sin LAT \sin DEC\right),$$

Where LAT is the latitude, DEC is the declination, GSC is the solar constant, n is the number of the mid-month day, and ω_s is the sunset hour angle. ω_s is calculated using:

$$\omega_s = -\tan LAT \tan DEC.$$

Then, the diffuse proportion, which is the fraction of radiation that has been scattered over all parts of the sky, is calculated using:

$$DP = \frac{GR - DR}{GR},$$

where GR is the global radiation and DR is the direct radiation.

The solar radiance is calculated by the ArcMap toolbox in ArcGIS and then quantified to rooftop areas only. This case study method is relatively general since many details of assumptions and

sources of data are not clear enough. However, it does provide sufficient detail for estimating solar radiation.

The literature review for calculating solar radiation simply provides background knowledge, such as theory and factors to consider, to the audiences but will not serve as a critical reference for the method since ArcGIS pro has its geoprocessing tool for estimating solar radiation. The Area Solar Radiation tool provides enough accuracy with relatively less calculating time for this study, and hence other complicated methods will not be considered.

Chapter 3: Background

3.1 Origin of solar PV panel

PV (photovoltaic) material can harvest solar energy and convert it into electrical energy. An individual unit of PV material is called a solar cell, which is made of different semiconductor materials. The typical power of a solar cell is one to two watts(*Solar Photovoltaic Technology Basics*, n.d.), which is not enough to drive even household appliances. However, by connecting solar cells into a chain or series, a larger unit called a solar module or pane can be produced to generate greater power.

Although the wide adoption of solar photovoltaic panels did not occur until the 21 century, the innovation and development of solar technology can be traced back hundreds of years ago. In 1839, French physicist Alexandre-Edmond Becquerel observed that electric currents were generated when the light hit the metals while working with metal electrodes in an electrolyte solution. However, this phenomenon could not be explained during that time (*This Month in Physics History*, n.d.). Then, Willoughby Smith discovered the photoconductivity of selenium in 1873 while testing materials for underwater telegraph cables, which indirectly led to the invention of the first solar cells from selenium in 1883 by American inventor Charles Fritts (*This Month in Physics History*, n.d.). One advancement was made by Russell Shoemaker Ohl, a semiconductor researcher, in 1940. He accidentally discovered a p-n junction (which will be discussed later) on a silicon sample that he was studying. The current was detected in that silicon sample when the light hit it. That particular sample has a crack in it, which "marked the boundary between regions containing different levels of impurities, so one side was positively doped and the other side negatively doped" (*This Month in Physics History*, n.d.). Therefore, an electric field was created because excess positive and negative charges were allowed to build

upon the two sides of silicon. This discovery is significant since modern solar PV panels rely heavily on p-n junctions. It directly led to the creation of the first practical silicon solar cell by the lab that Ohl worked for, Bells lab (*This Month in Physics History*, n.d.). Not until 1954, after trying many different combinations of impurities, they finally found boron-arsenic silicon cells, which solved many problems they had encountered. The solar cells they created had a conversion efficiency of six percent, which was much higher than the previous solar cell with one percent efficiency (*This Month in Physics History*, n.d.). However, the process of "recreating the accident" and stabilizing the technology to be used practically required years and the hard work of scientists.

3.2 Development of the Solar Panel

"Support for R&D and photovoltaic technology change are crucial aspects in accelerating the widespread adoption of photovoltaic systems" (Sampaio & González, 2017).

Energy is directly related to people's quality of life and industrial production in modern society. With the increasing population on the earth, the energy demand has increased for many years. Yet the burning of traditional fossil fuels has led to man-made climate change. To sustain the increasing energy demand without contributing to carbon emissions, people have recognized the importance of renewable energy in the past decade, especially solar energy, due to its accessibility. As a result, the PV market has been explored worldwide, especially in Europe, China, and the United States. It has proliferated from 2000 to 2015 with a growth rate of 41% because of high levels of investment (Sampaio & González, 2017). The major development of the solar PV industry is reflected in material use, energy consumption to manufacture these materials, device design, and production technologies (Parida et al., 2011; Razykov et al., 2011; Sampaio & González, 2017).

3.2.1 Technology development

The modern solar PV utilizes the semiconductor material, which has a valence band and a conduction band, to convert solar energy to electricity. The valence band has the presence of the electron, whereas the conduction band does not have electrons. When enough light hits the semiconductor, the solar energy could trigger the movement of electrons from the valence band to the conduction band and thus create a current. The interface between two semiconductor material types is called the p-n junction formed by the method of doping. The current across the junction can be created when the holes from the p-side diffuse to the n-side and the electrons from the n-side diffuse to the p-side.

Solar PV technologies have become very diverse because of decades of development (Subtil Lacerda & van den Bergh, 2016). The ideal material for solar PV should have a relatively low bandgap, between 1.1-1.7 eV. It should be non-toxic, accessible, suitable for long-term use, and able to conduct large volume production (Sampaio & González, 2017). However, it is impossible to find a material that fits all the requirements (Goetzberger et al., 2003). The most common semiconductor used in solar PV is silicon, which has a bandgap of 1.12eV. The first generation of commercial solar PV utilizes the technology of crystalline silicon (c-Si). It can be divided into two forms: a simple form called crystalline form (sc-Si) and multi-crystalline form (mc-Si) (Sampaio & González, 2017). The second generation is the thin-film photovoltaic technologies which have three categories: (1) Amorphous silicon (a-Si) and micro amorphous silicon (a-Si /μc-Si); (2) cadmium telluride (CdTe); and (3) copper indium selenide (CIS) and copper, indium gallium dieseline (CIGS) (Sampaio & González, 2017). The third generation is the organic PV cells, but this technology has not been commercialized (Sampaio & González, 2017). There are many other solar technologies on the market, such as dye-sensitized solar cells

, and each of them has advantages for different applications.

Besides the diversity of solar technology, the increasing conversion efficiency also drives the widespread adoption of solar PV. In figure 5, it is easy to observe a general increasing trend for all kinds of solar technology, especially the Multi-junction concentrator solar cells and the organic solar cells.

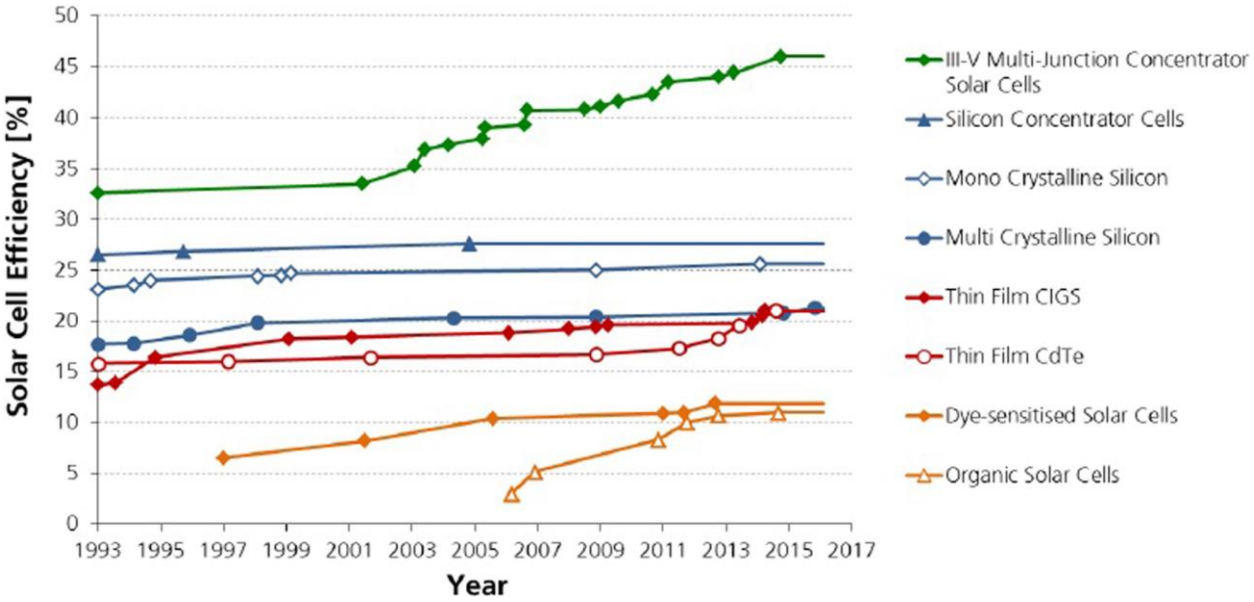

Figure 5:The change in the efficiency of solar cells.

Source: Data: Solar Cell Efficiency Tables (Versions 1–47), Progress in Photovoltaics: Research and Applications, 1993–2016. Graph: Simon Philipps, Fraunhofer ISE 2016

3.2.2 Economic and political factors

The thrust of subsidies, tax breaks, and other financial incentives are also crucial for the development and broad adoption of solar PV (Devabhaktuni et al., 2013; Sampaio & González, 2017). Two common political strategies motivate the solar PV market to grow. The first kind is feed-in-tariff (FIT), which encourages the investment of renewable installations on an individual scale. This mechanism is widely used in Germany, Denmark, Spain, and China (Sampaio & González, 2017). It is noticeable that China has 71 % of the market share among individual

consumers at the end of 2015 (Sampaio & González, 2017). The second kind is the Renewable Portfolio Standard(RPS), which requires a certain amount of energy consumed to be generated from renewable sources. This regulation is commonly used in the United States, United Kingdom, Japan, and Sweden (Sampaio & González, 2017). For example, The Goleta City Council has pledged to adopt a goal of 100 percent renewable electricity for all municipal facilities and community-wide electricity supply by 2030 and meet at least 50 percent in 2025. To meet this goal, adopting solar PV panels is unavoidable.

Another economic factor is the decrease in the price due to the increasing volume of production and the decreasing cost of manufacturing (Sampaio & González, 2017). A consistent reduction in price can be observed in figure 6 with some fluctuations.

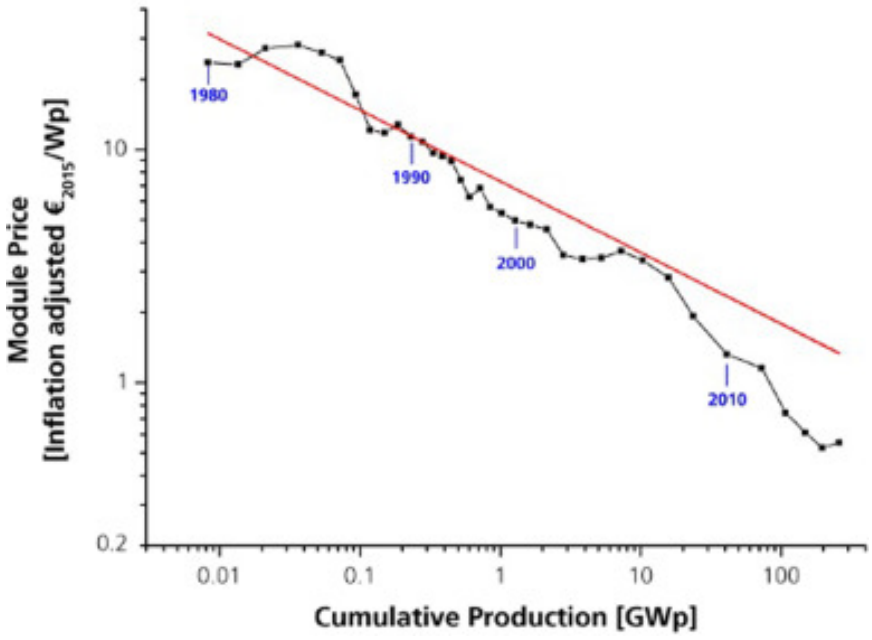

Figure 6:The change in the price of solar Module

Source: Data: from 1980 to 2010, estimation from different sources: Strategies Unlimited, Navigant Consulting, EUPD, pvXchange; from 2011 to 2015: IHS. Graph: PSE AG 2016.

Moreover, the benefits of solar PV panels make it stand out among other renewable energy generation. Some benefits include low cost of operation and maintenance, free and clean energy source, higher availability, close to the consumer, environmentally friendly, and noiseless (Sampaio & González, 2017). Combined with the factors mentioned above, the market share of solar PV panels has decentralized for many years. Although it does have some limitations, such as the high dependence on the geological location because of the solar irradiation and high initial cost, the disadvantages can be offset by benefits.

3.3 Community solar

3.3.1 What is community solar?

While the criticism of the renewable energy system as mentioned above remains and most of the attention is drawn from the utility-scale project and individual projects, the community solar system provides huge potential to transfer to a more sustainable and reliable energy system (Peters et al., 2018). The U.S. Department of Energy defines community solar as "any solar project or purchasing program, within a geographic area, in which the benefits of a solar project flow to multiple customers such as individuals, businesses, nonprofits, and other groups. In most cases, customers are benefitting from energy generated by solar panels at an off-site array" (*Community Solar Basics*, n.d.). Given the definition from the U.S. Department of Energy, however, (Seyfang et al., 2013) and (Peters et al., 2018) claim that there is no universal definition for the community, which can cause inconsistency in assessing the effectiveness "through appropriate regulatory and policy frameworks" when community solar is commonly regarded as a strategy to reduce carbon emission for a community. In fact, what exactly community renewables do and should mean is always a hot topic of discussion in this field, and there is no standard definition present (Brummer, 2018; Walker & Devine-Wright, 2008).

Among the 12 projects that Walker and his colleague have examined, most of them interpreted the "community" in quite different ways. To be specific, it can generally be categorized into three kinds. The first type believes that community means a project is led by organizations "with a charitable status and without commercial interests." The second type identifies community projects as ones that "involve public buildings used by members of the community". The last one recognizes the significance of the involvement of local people and "having a direct financial stake in a project through cooperative share issues" (Walker & Devine-Wright, 2008). Instead of strictly defining community solar, (Seyfang et al., 2013) states that community solar refers to many initiatives, including but not limited to "locally-owned renewable energy generation, community hall refurbishments, and collective behavior change programs." Meanwhile, (Walker & Devine-Wright, 2008) has come up with a two-dimension theory, which focuses on process and outcome. In this theory, the subject of the project is essential. The "process" raises the question of who owns and manages the project? Who is influenced (benefited) from the project? The "outcome" concerns who is the project for? What are the benefits? This theory is also recognized by (Peters et al., 2018).

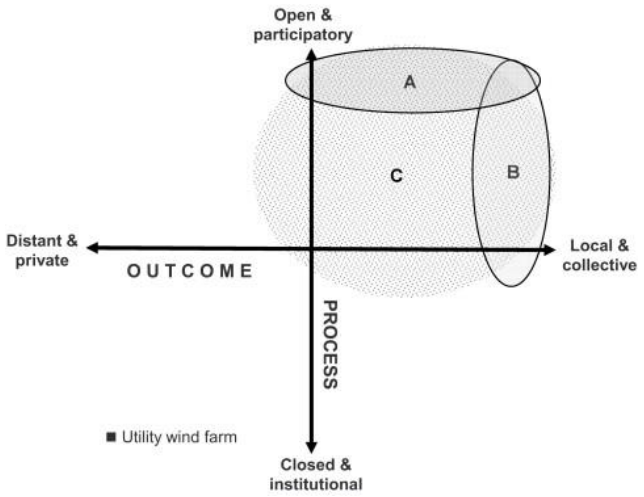

Figure 7:The process and outcome dimensions for community solar proposed by (Walker & Devine-Wright, 2008).

A community project should fall into the top region of this graph. Region A heavily emphasizes the involvement of local people, which could include the construction, management, and running of the facility. Region B focuses more on the outcome, such as the distribution of benefits, with less concern about the participants. Some advantages could be educational resources and job opportunities. From the author's view, Region C is more expansive and flexible since people emphasize the progress that leads to something "productive and useful."

Considering the flexible definition of the community solar program, the study site, Isla vista, has one community solar program started by ISLA VISTA FOOD COOPERATIVE in 2017. This organization aims to "provide the residents of Isla Vista and neighboring communities of Santa Barbara County with reasonably priced foods, products and services that promote a healthier lifestyle and environment" (Isla Vista Food Cooperative | RE-Volv, n.d.). The organization built a program with a 25 kW solar system. Although the community does not directly consume the electricity generated from this system, the organization used the savings from the electricity bills to benefit the community, such as producing low-cost, organic food, participating in more food distribution programs, and hosting more community engagement and educational events(Isla Vista Food Cooperative | RE-Volv, n.d.). Given the fact that the major participants of the organization are local residents, and the product goes to the local community, the program mentioned above could be defined as a community solar project in Isla vista. Even though there is only one existing community solar program, and the residents are benefiting indirectly, building community solar projects in Isla vista has great potential to reduce carbon emissions and benefit a large number of residents due to the high population density in Isla vista.

3.3.2 Benefits and Inadequacies of Community Solar

The number of shared solar programs has grown from one in 2006 to 41 as of August 2014, as it has proven its contribution to fighting climate change and its users (Peters et al., 2018). Such contributions also include economic benefits, education and acceptance, participation, community building and self-realization, renewable energy generation targets, and innovations (Brummer, 2018). Economic benefits usually refer to the income for local communities in the form of direct financial gains and indirect regional economy simulation (Brummer, 2018). Specifically, the direct benefits are presented as revenues from energy sales or land rent tax revenues, while the major indirect economic benefits are providing employment during the construction and management of the facilities. Community solar projects can also increase people's understanding and acceptance of solar panels and other renewable energy. Participating in a solar community program in any role allows people to understand the working theory and technical details of solar PV, electricity transmission, and storage (Hoffman & High-Pippert, 2010). Moreover, the studies in this field have shown people's general increasing awareness of energy issues such as generation and consumption, which can lead to more sustainable saving behavior and more participation in clean energy activities. According to (Brummer, 2018), "clean energy activities are mentioned to help create trust in RE generation, helping it to be better accepted." Collectively, the benefits mentioned above can affect people's perception of climate change and their lifestyles (Hoffman & High-Pippert, 2005). What's more, people involved in community solar programs are less likely to reject man-made climate change effects (Hoffman & High-Pippert, 2005). Also, community programs give their residents more flexibility to make decisions, thus increasing their interest in community activity and building a

pronounced identity. The community solar program can relieve the pressure of meeting the renewable energy generation target (Brummer, 2018).

However, while the benefits of community solar may drive its development, the inadequacies could be why community solar programs are not as popular as individual solar panels. The barriers are often related to the economic factors and legal framework. Many renewable energy cooperatives are small, making it hard to afford the required resources for the project, such as time, expertise, the initial cost of construction, and paid jobs (Brummer, 2018). As a result, the community solar projects heavily relied on volunteer work. The legal process for a project to get permission is also complex. A general consistent political regulation is missing, making it even harder to start a project when considering the effort of researching and planning (Aylett, 2013). Besides that, some community projects need to face competition and discrimination from the large energy companies because they fight actively against renewable energy generation (Sovacool & Lakshmi Ratan, 2012). The competition makes it hard for small cooperatives to get loans and funding for maintenance, even if they have money to start the project. Given the best situation in which the obstacles mentioned above can be resolved, other potential difficulties include the saturation effect. This is a genuine factor that planners must consider since the best suitable place for PV installation might have already been possessed (Brummer, 2018). For the target site of this analysis, the high density of residential land use might lead to insufficient space for community solar programs, or small-scale solar panels might take the good spots. Meanwhile, high population density is also an opportunity for community solar programs since it has a higher potential to benefit a large number of people.

In conclusion, the effort to harvest solar energy has been made since the 1800s, and the great demand of the market associated with rapid development and low cost has led to the

worldwide distribution and utilization of solar technology. While the individual scale solar program might be expensive to start and the payoff period could be relatively long, the community solar program provides the huge potential for reducing carbon emissions in the energy sector with low cost per user. However, there is no clear definition of community solar, and the debate has never stopped. Generally, it can be classified into three groups, the first type focuses on the involvement of local people, the second group focuses on the distribution of benefits, and the last one lies somewhere between the first two. Community solar is commonly recognized for its superiority, including economic benefits, education, and acceptance for local people, participation, community building and self-realization, renewable energy generation targets, and innovations. But the limitation, such as the incomplete legal regulation and the competition from the large energy companies, are some of the main reasons there are not many large community solar programs.

Chapter 4: Findings

4.1 Result and Analysis

This chapter makes an effort to convert raw LiDAR data to interpretable images and tables to help the audience, especially those who are not familiar with the energy field and ArcGIS Pro, understand the result. The rasters and tables that are generated by using the procedure described in the method section will be shown and analyzed in detail. To be specific, the audience will be able to see how the data is processed only to get desired features; what are the parameters that can remove the unwanted data; how the rasters are linked like a chain, which the output raster generated from the last step could be used as an input raster for next step; and finally and the most importantly, a visualization of the results which the audience is able to see a gradually decreasing of the suitable area for solar PV installation. However, not all purposes proposed at the beginning of the study are achieved due to some objective factors, and there are also some limitations, which will be discussed in this chapter as well.

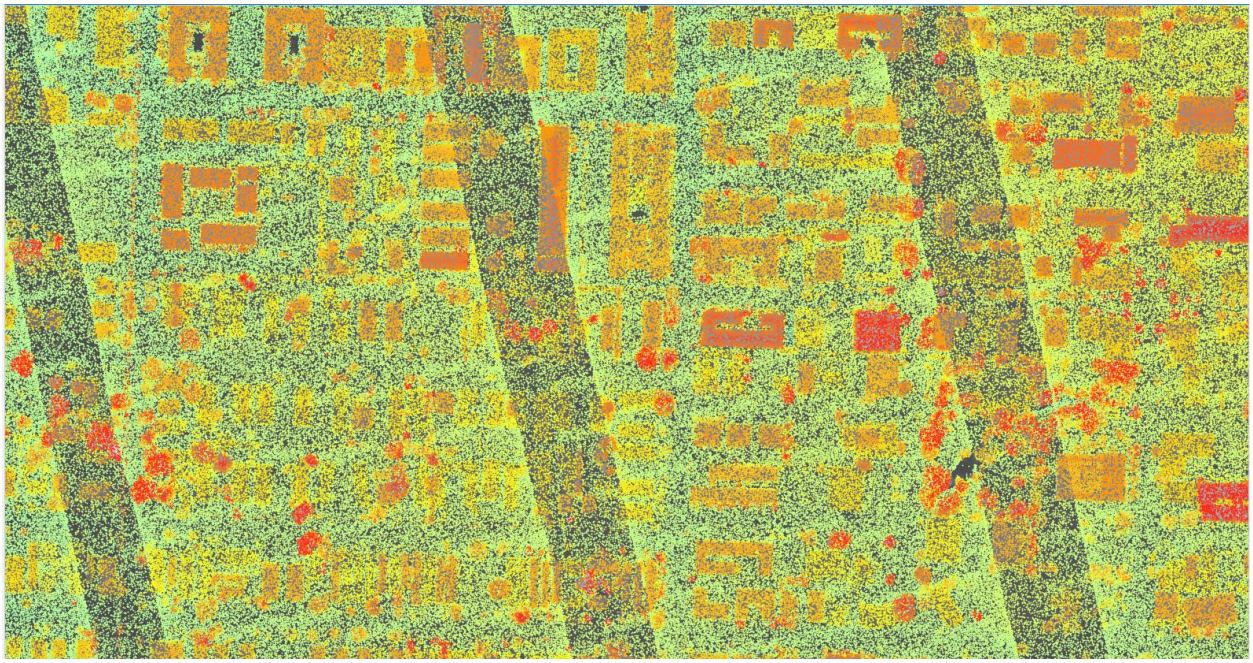

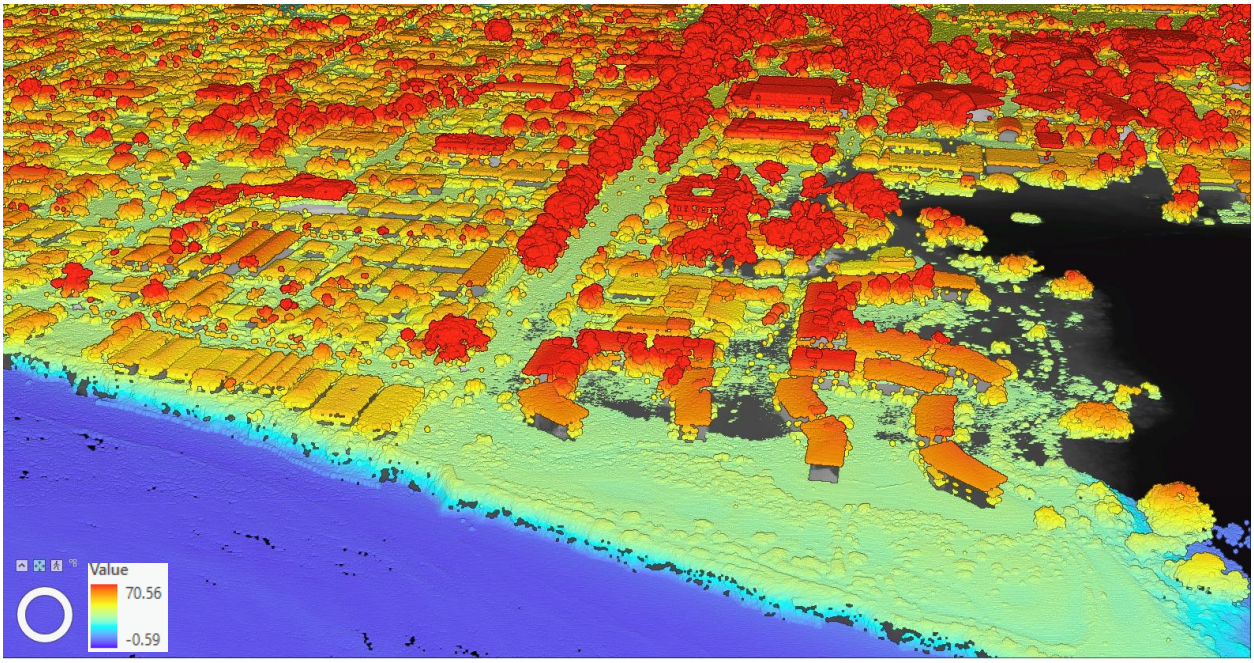

Figures 8(a) and 8(b): Visualization of the LiDAR data.

8(a) is the 2D view of the LiDAR point cloud in the study area, and 8(b) is the 3D view of the LiDAR points. The points with high elevation are shown in dark red, and points with low elevation are shown in green and blue. The raw LiDAR data contains many undesirable points that represent the environment like trees, water, and even cars on the street. Those points are useless for the analysis and should be removed. The useful points are gone through a series of classification and separation.

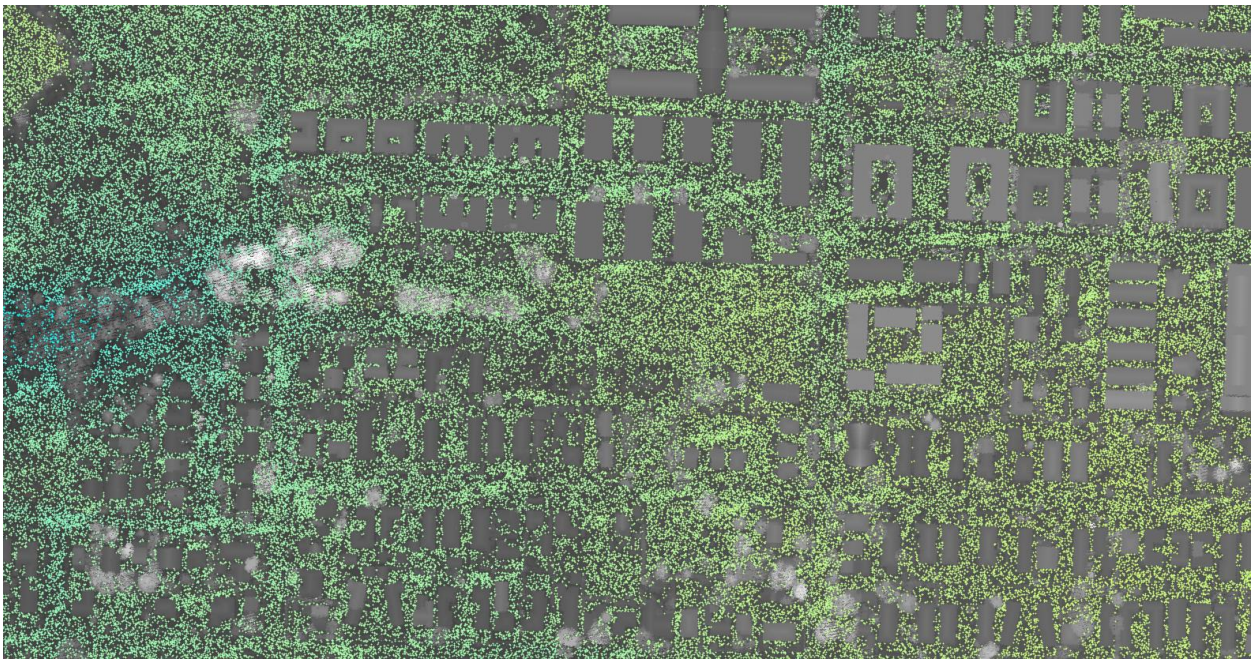

Figure 9: The LiDAR points after the ground classification.

It is clear to see that the points in this image only show the ground. It is important to note that the Classify LAS Ground tool does not remove points indicating other features; instead, it just creates a new group showing all points that represent the ground. This means the user can still see others features by checking/unchecking the box representing each feature. The ground points are necessary to create DEM.

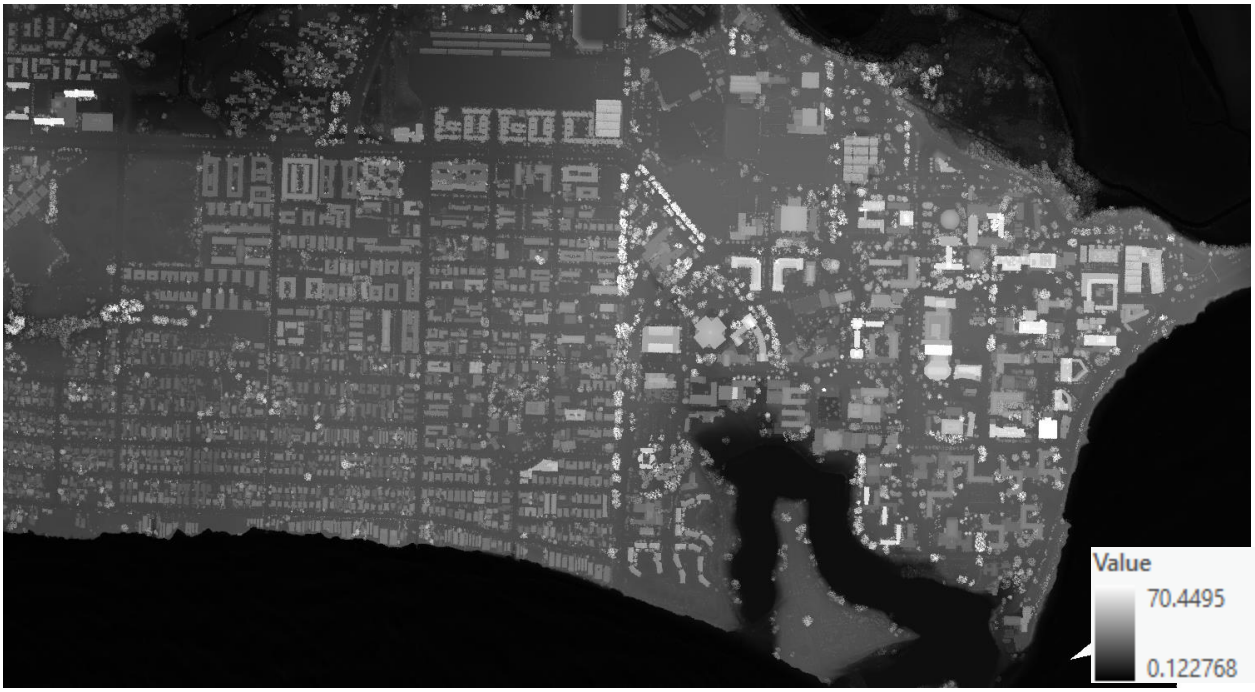

Figure 10:The digital elevation model (DEM).

The digital elevation model (DEM) is generated from the ground LiDAR points using the LAS Dataset To Raster tool. The dark areas represent low elevation, and the light areas represent high elevation. The DEM is a crucial input layer for subsequent image processing.

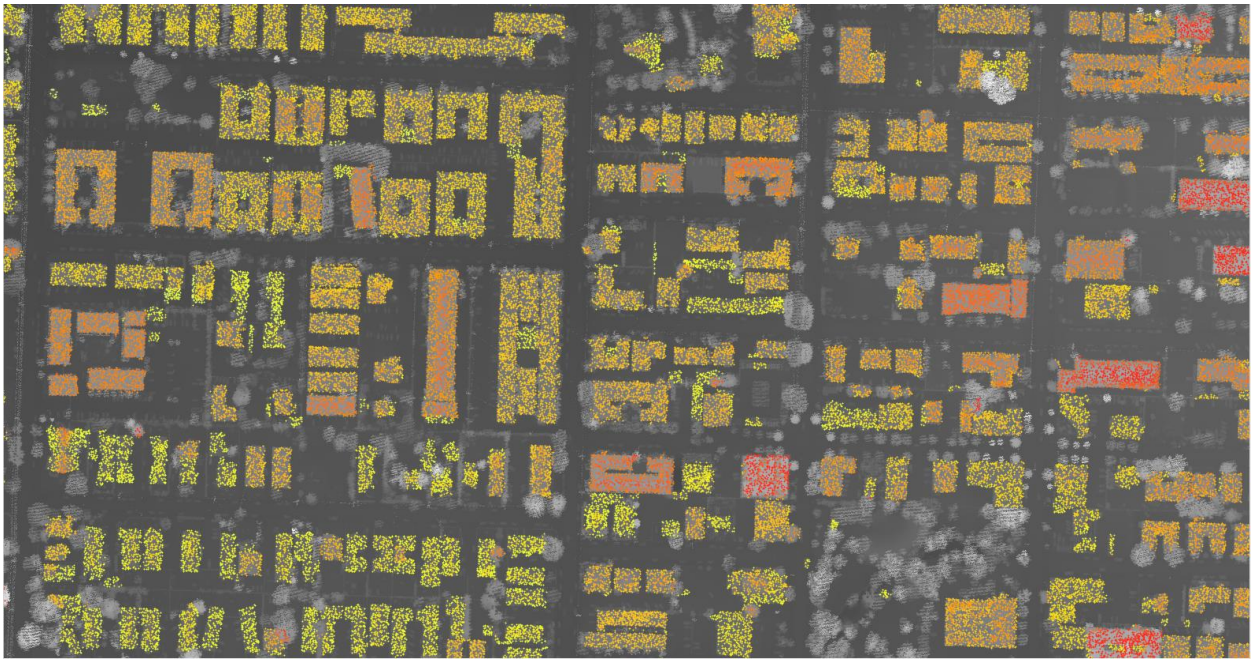

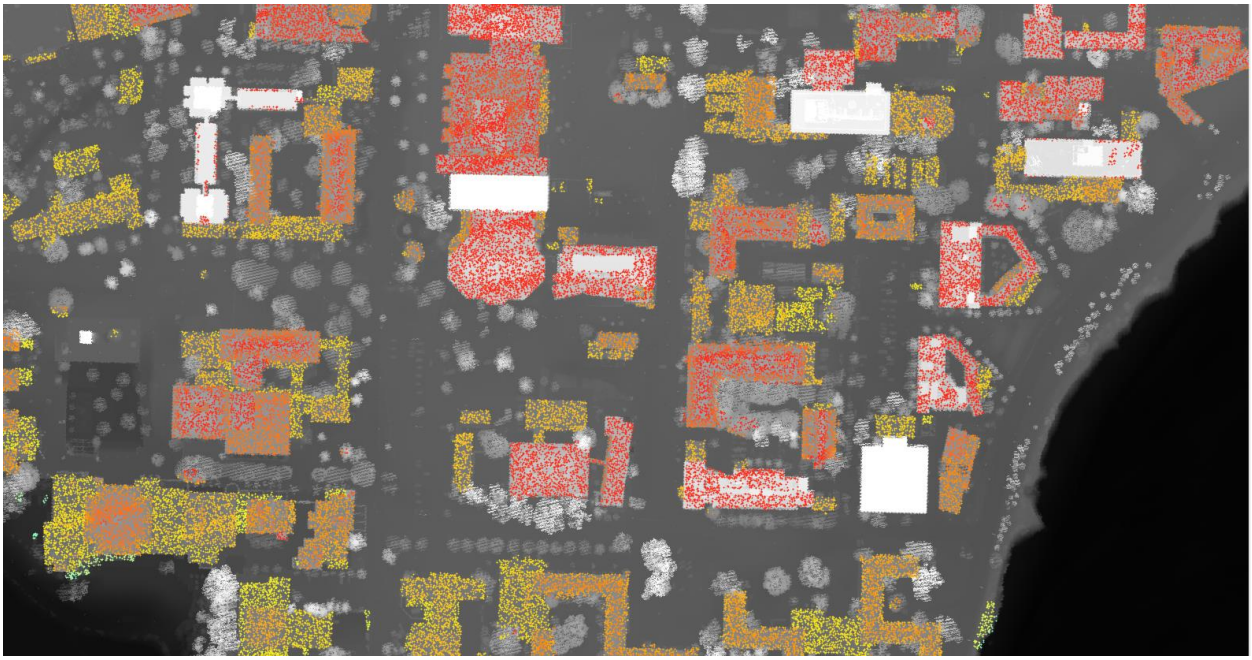

Figures 11(a) and 11(b): The LiDAR points that only represent the buildings.

Figure 11(a) shows the UCSB campus, and 11(b) shows Isla Vista. Note that the Classify LAS building tool is used after an aggressive cleaning process using Classify LAS Noise tool. The benefit of using an aggressive clean process with a low cut-off value is fewer noise points and outliers. However, the drawback is that the points of some tall buildings on the UCSB campus are not included. Nevertheless, this phenomenon does not occur in Isla Vista because of the low building elevation. This missing building will be recaptured when making the building footprint. The reason for applying this strategy is that it is tough to remove all the noise manually, while it

requires relatively less effort to reconstruct the missing building footprints.

Figures 12(a) and 12(b): Raw building footprint.

Figure 12(a) is the building footprints generated from the LAS Point Statistic As Raster tool. The majority of buildings are captured and correctly represented. However, some areas are

misidentified as buildings, which are mainly concentrated along the coast, and there are also holes in the polygons. The holes within the polygons can lead to a lower rooftop area than it actually is, which will impact the final result when calculating solar radiation and electricity production. Figure 12(b) is a zoom-in of the study area so that the hole of the building polygons can be seen. Also, note that the data of an area on the southern side of Isla vista along the coast is missing. This could result from cloud blocking and reflecting the beam to the sensor before it hits the ground.

Figure 13:The building footprint after the cleaning process and manual correction.

By setting parameters in the Select Layer By Attribute tool, the building polygons are regularized, as shown in the bottom left of the image. Although most of the holes are filled automatically, the rest of them will be carefully examined and corrected manually. Also, the buildings on the southern part of IV with missing data are also identified manually using the orthophoto as a reference, while the misidentified areas are removed.

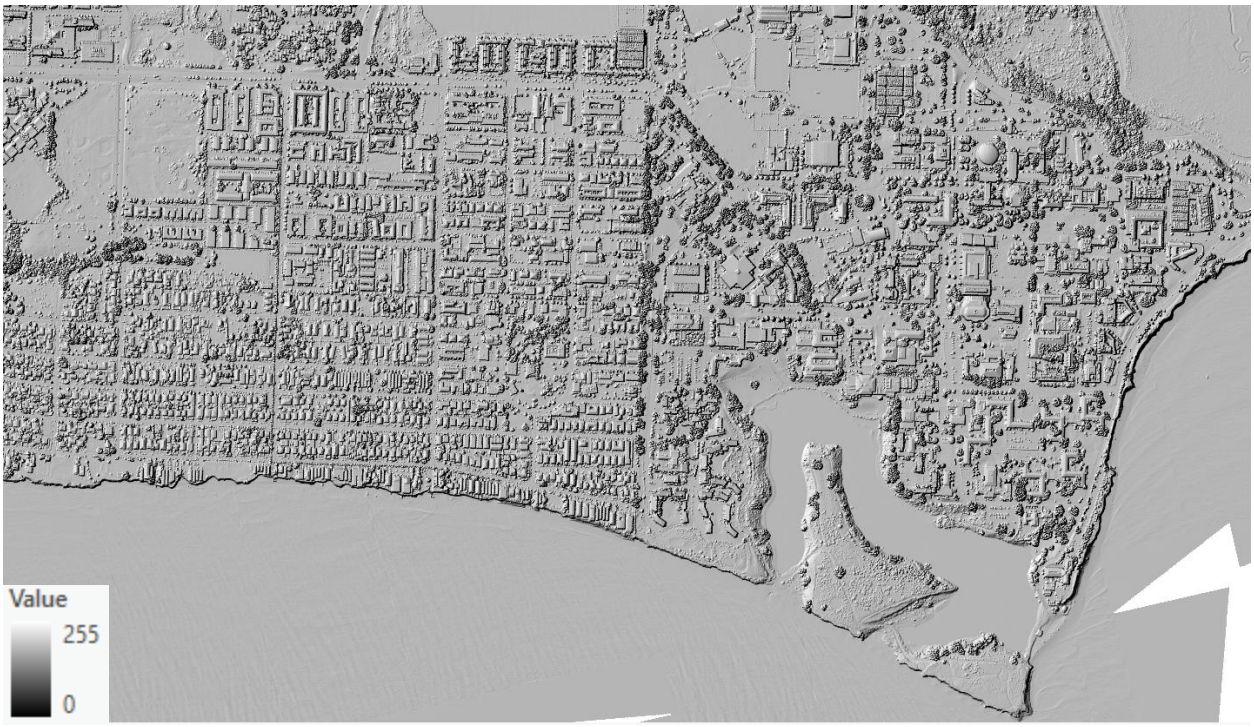

Figure 14: The grayscale 3D representation of the terrain surface using the Hillshade tool.

The analysis of shadow is done by considering the effects of the local horizon at each cell. Raster cells in shadow are assigned a value of zero. Shadow is observable mainly in the tree canopy and on the roof edge, whereas most rooftops are not in shadow. This is because the average building elevation is not high, and there are no extremely tall buildings that can block the surrounding environment. Apparently, the raster cells that are in shadow do not have access to the incoming solar radiation. Thus, those areas are not considered suitable for solar PV installation.

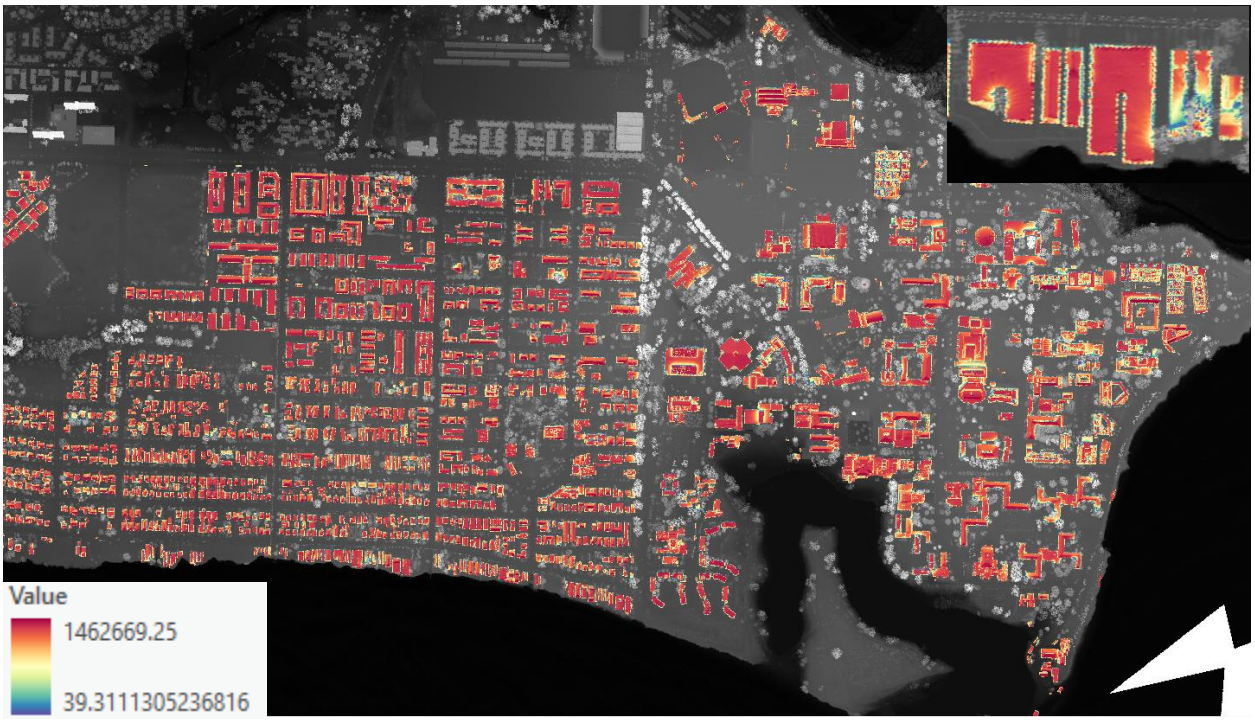

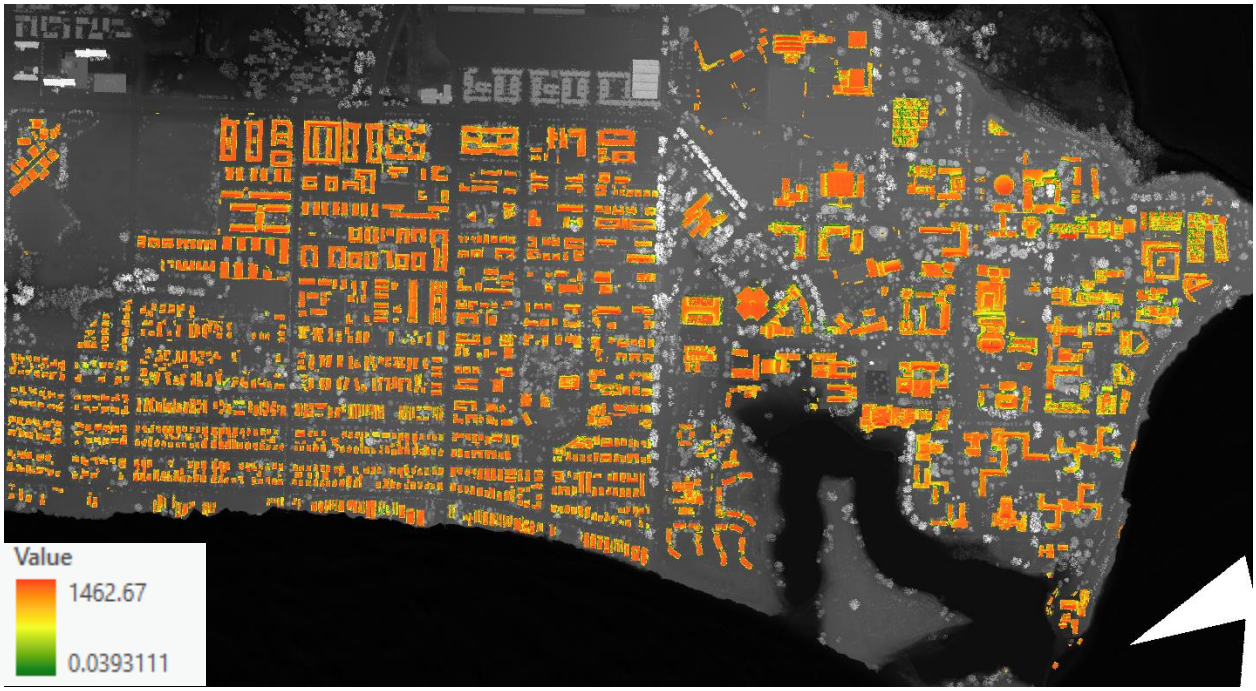

Figures 15(a) and 15(b): The solar radiation was calculated by the Area Solar Radiation tool.

Note that only solar radiation is only calculated for buildings because the raster of building footprints is used as a mask. This auto-generated raster is in watt-hours per square. To make the

raster easy to read, the unit is converted to kilowatt-hours per square meter(kWh/m2) by dividing the value by 1000. Two different symbologies are applied to differentiate the raster. Note that the buildings on the top right of Figure 15(a) are a zoom-in of the raster.

Figure 16: The slope raster of the study area is created by the Surface Parameters Tool using DEM as input.

The darker the color, the higher the slope. This raster is helpful as one of the necessary parameters to eliminate unsuitable roofs. Note that the ArcGIS Pro automatically divides the slope into 11 groups to make the differences more visible in the raster. However, only 10 and 45 degrees are essential for the analysis since any degree below ten would be considered flat, and any degrees greater than 45 would be considered too steep.

Figure 17: The aspect raster of the study area generated using the Surface Parameters tool.

The standard categorization of the aspect is: (a) North: 337.5- 22.5 degree; (b) Northeast: 22.5-67.5 degree; (c) East: 67.5-112.5; (d) Southeast: 112.5-157.5 degree; (e) South:157.5-202.5 degree; (f) Southwest: 202.5-247.5; (g) West: 247.5-292.5 degree; (h) Northwest: 292.5-337.5 degree. The aspect raster will be used as input raster to remove areas facing north (with an aspect value between 300-60).

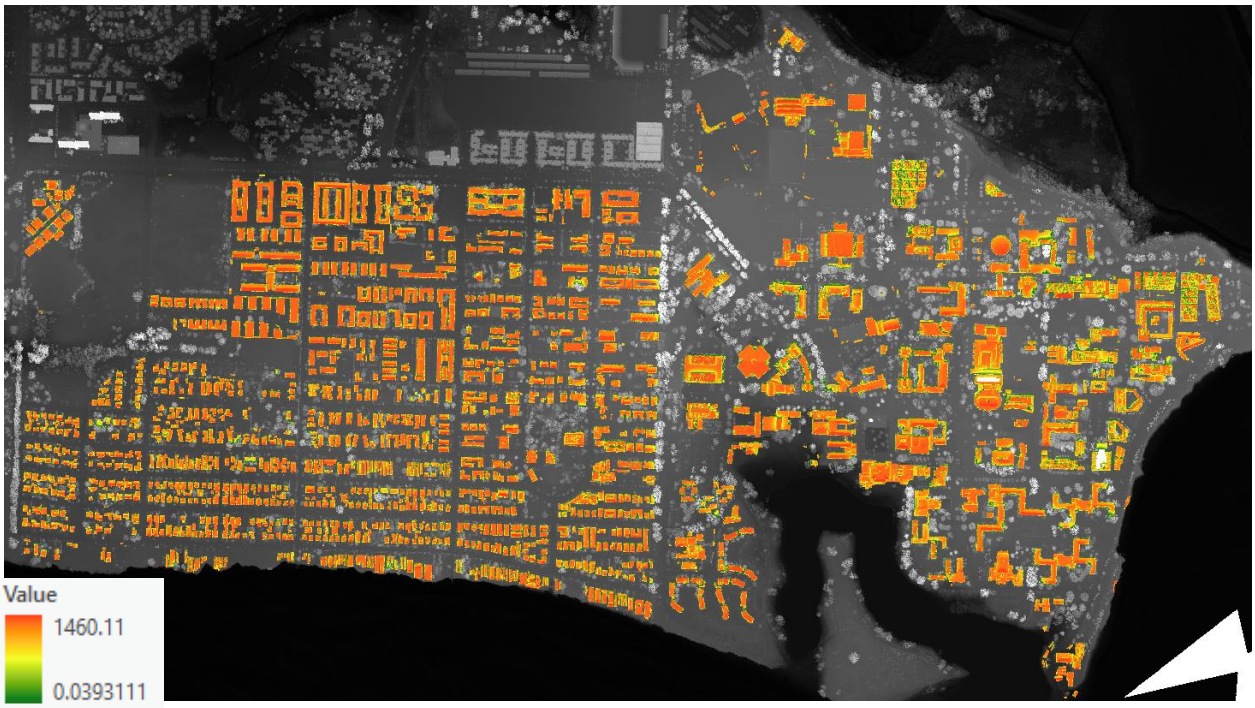

Figure 18: The solar radiation raster in which the areas with slopes higher than 45 degrees are removed.

There is little change compared to the [kwh image] since almost all buildings have a slope of fewer than 45 degrees. Moreover, it is easy to observe that the environment, such as trees, usually has a larger slope. However, since the calculation was not applied to the environment due to the mask of building footprints, it is reasonable to see little change in this step.

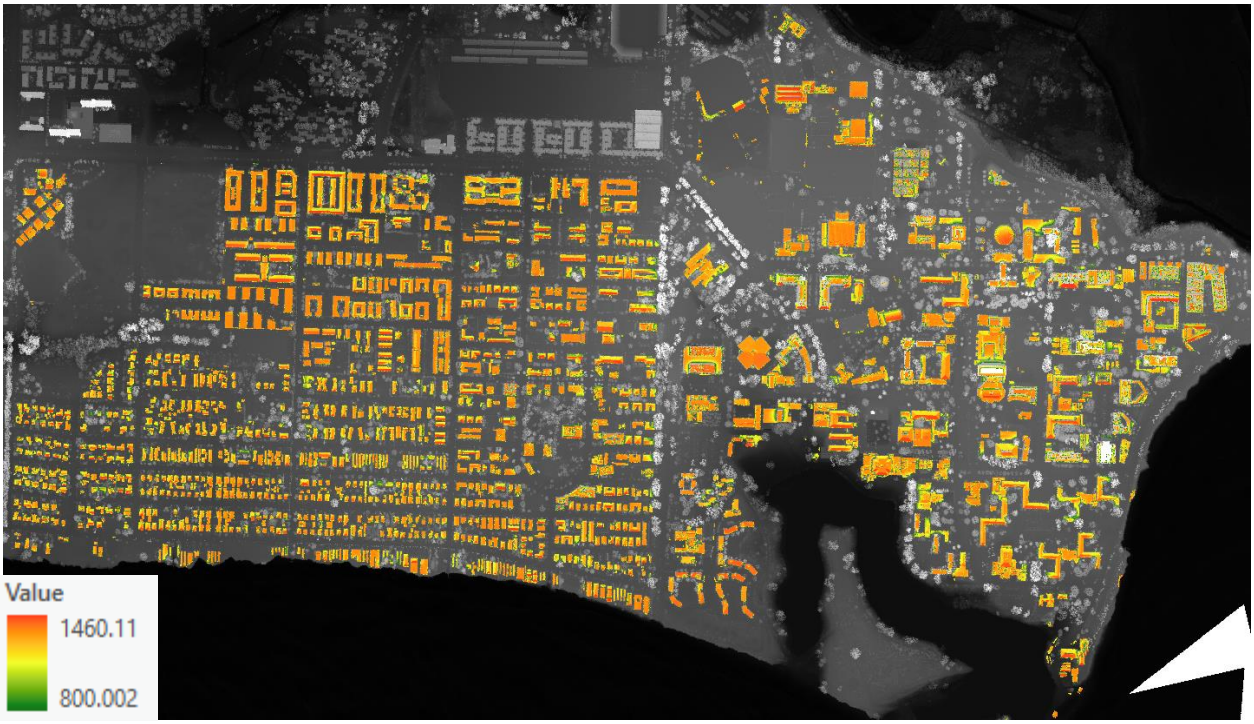

Figure 19: The solar radiation raster after the removal of an area with incoming solar radiation less than 800kWh/m2 by the Surface Parameters tool.

Although there is an observable change in color in the raster, there is actually no significant difference from the previous raster. This is because by changing the lower limit to 800 kWh/m2, the color bar is scaled up, which causes the overall color to be lighter. However, the solar resource is abundant in the study area, as mentioned in the first chapter, and it is rare to see areas with low incoming solar radiation.

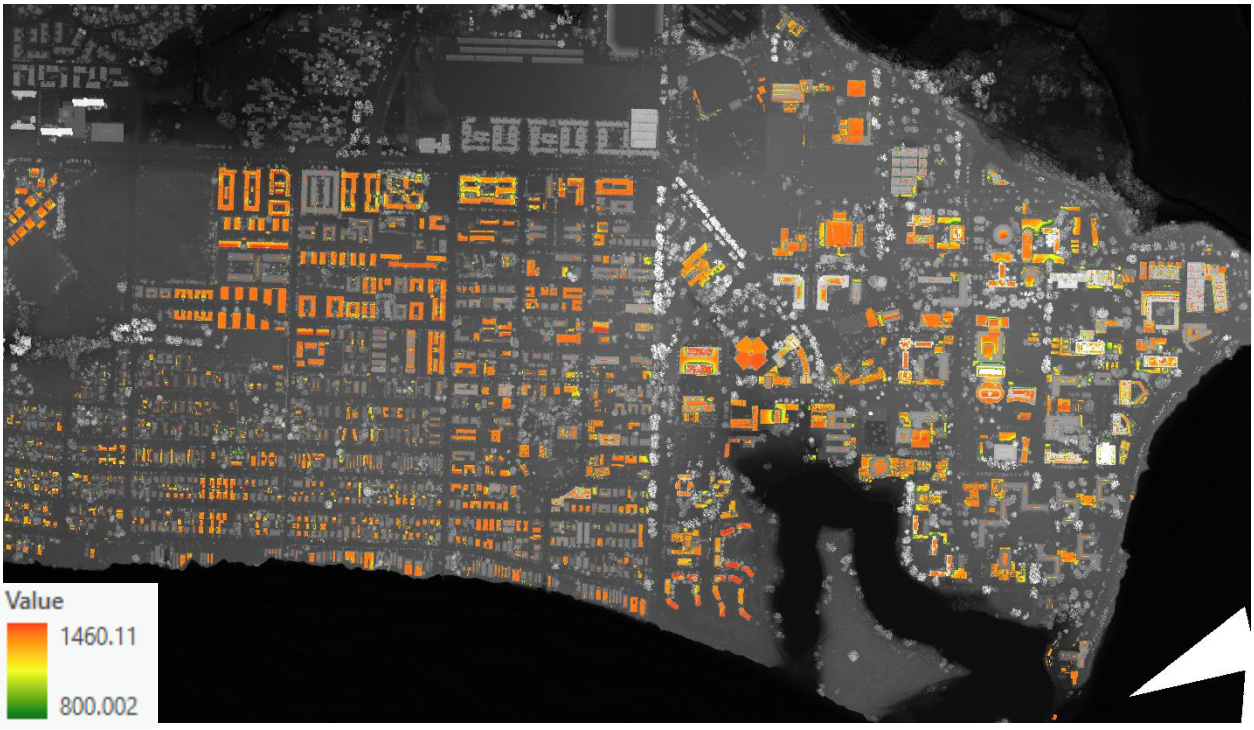

Figure 20: The solar radiation raster only shows areas with slopes less than 10 degrees.

A significant number of buildings are not observable in this raster since most multi-dwelling units do not have flat roofs. This raster is created to serve as a false raster to calculate the final solar radiation.

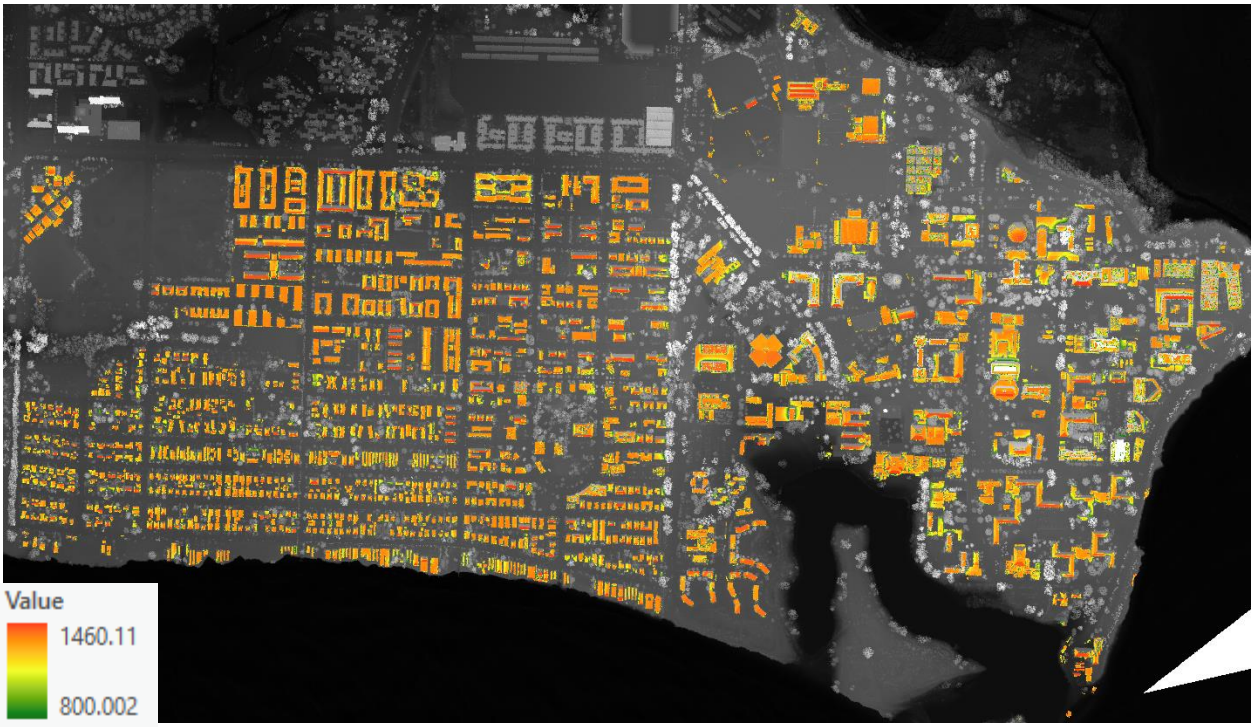

Figure 21: The final solar radiation raster.

The areas that are facing north, with an aspect value between 60 and 300, are removed. Then, this raster is imported as a true raster in the Con tool with the solar radiation raster that only shows areas with a slope less than 10 degrees as a false raster to calculate the final solar radiation. As a result, the false cells are replaced by values from the low slope layer, and the output layer will contain both areas that do not face north and areas with a low slope. These areas are ideal roofs for solar PV installation.

Solar_Rad_Table

Field: Add Calculate | Selection: Select By Attributes Zoom To Switch Clear Delete Copy | Rows: Insert

	OBJECTID *	Id *	COUNT	AREA	MIN	MAX	RANGE	MEAN	STD	SUM
1	1	12046	23	5.75	831.423706	1106.737061	275.313354	981.375992	67.1753	22571.647827
2	2	12106	64	16	819.305298	1416.084473	596.779175	1194.342503	170.349726	76437.920166
3	3	12113	1243	310.75	803.967529	1432.814453	628.846924	1277.360184	119.954531	1587758.708923
4	4	12119	455	113.75	801.687317	1394.473267	592.78595	1195.108989	145.107941	543774.589844
5	5	12130	3264	816	800.597351	1430.136108	629.538757	1260.644638	144.45133	4114744.097229
6	6	12134	46	11.5	901.640076	1449.793213	548.153137	1325.827296	128.149695	60988.055603
7	7	12137	374	93.5	803.347229	1422.939453	619.592224	1185.266063	158.210548	443289.507446
8	8	12143	1541	385.25	802.168091	1417.648804	615.480713	1289.783181	115.060374	1987555.881714
9	9	12187	48	12	804.078308	1171.492798	367.41449	1015.845437	108.252961	48760.580994
10	10	12199	662	165.5	800.262512	1426.95813	626.695618	1209.276563	143.429968	800541.084412
11	11	12209	293	73.25	801.684509	1363.340088	561.655579	1306.505123	95.837533	382806.000977
12	12	12242	4362	1090.5	800.045837	1418.295044	618.249207	1201.427009	134.238214	5240624.613892
13	13	12243	82	20.5	801.808655	1364.088257	562.279602	1115.926483	148.951139	91505.971619

0 of 934 selected | Filters: | 100%

Table 1: The solar radiation table.

The table produced by the Zonal Statistics as Table tool only has four elements: Building_ID, COUNT, AREA, and MEAN. Each unique building has a Building_ID. COUNT represents the number of suitable cells for that building. AREA gives the area covered by suitable cells in m2, and MEAN the average solar radiation in (kWh/m2) that these cells receive. However, since the table is independent of the solar radiation raster, they have to be joined together using the Join Field tool to view the statistics on the map. See complete table in:[https://docs.google.com/spreadsheets/d/1SHnMY-LO59fbGGN5OrQnCuWAHzLPa1Bp/edit?usp=sharing&ouid=117252232660339936296&rtpof=true&sd=true]

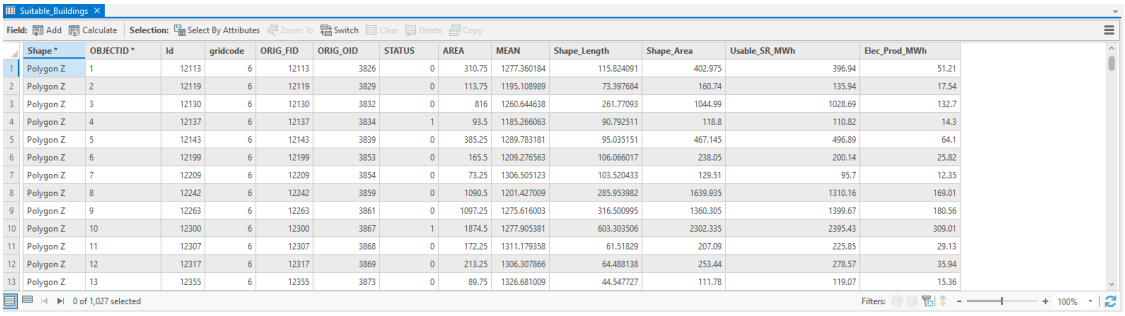

Suitable_Buildings

	Shape *	OBJECTID *	Id	gridcode	ORIG_FID	ORIG_OID	STATUS	AREA	MEAN	Shape_Length	Shape_Area	Usable_SR_MWh	Elec_Prod_MWh
1	Polygon Z	1	12113	6	12113	3826	0	310.75	1277.360184	115.824091	402.975	396.94	51.21
2	Polygon Z	2	12119	6	12119	3829	0	113.75	1195.108989	73.397684	160.74	135.94	17.54
3	Polygon Z	3	12130	6	12130	3832	0	816	1260.644638	261.77093	1044.99	1028.69	132.7
4	Polygon Z	4	12137	6	12137	3834	1	93.5	1185.266063	90.792511	118.8	110.82	14.3
5	Polygon Z	5	12143	6	12143	3839	0	385.25	1289.783181	95.035151	467.145	496.89	64.1
6	Polygon Z	6	12199	6	12199	3853	0	165.5	1209.276563	106.066017	238.05	200.14	25.82
7	Polygon Z	7	12209	6	12209	3854	0	73.25	1306.505123	103.520433	129.51	95.7	12.35
8	Polygon Z	8	12242	6	12242	3859	0	1090.5	1201.427009	285.953982	1639.935	1310.16	169.01
9	Polygon Z	9	12263	6	12263	3861	0	1097.25	1275.616003	316.500995	1360.305	1399.67	180.56
10	Polygon Z	10	12300	6	12300	3867	1	1874.5	1277.905381	603.303506	2302.335	2395.43	309.01
11	Polygon Z	11	12307	6	12307	3868	0	172.25	1311.179358	61.51829	207.09	225.85	29.13
12	Polygon Z	12	12317	6	12317	3869	0	213.25	1306.307866	64.488138	253.44	278.57	35.94
13	Polygon Z	13	12355	6	12355	3873	0	89.75	1326.681009	44.547727	111.78	119.07	15.36

Table 2: The attribute table of suitable buildings.

The last step of selecting suitable buildings is eliminating any building with an area less than 30 m2. The features of the suitable buildings are exported to a table. However, the default table only has five fields: Building_ID, COUNT, AREA, MEAN, Shape_length, and Shape_Area. Shape_length indicates the parameter of the polygons and the Shape_Area is the area of the polygons. The extra two fields are not crucial for the analysis. A new field called usable solar radiation in MWh is added to the table. This field is calculated by (AREA * MEAN)/1000. The last step is converting solar radiation to power, calculated by (usable solar radiation * 0.15 * 0.86). The unique statistics of any building can be observed by clicking it on the raster, as shown in figure 22. See complete table in:

[https://docs.google.com/spreadsheets/d/1BvUMngbfBm16XmTpcGh8KNjGpRY5sRhM/edit?usp=sharing&ouid=117252232660339936296&rtpof=true&sd=true]

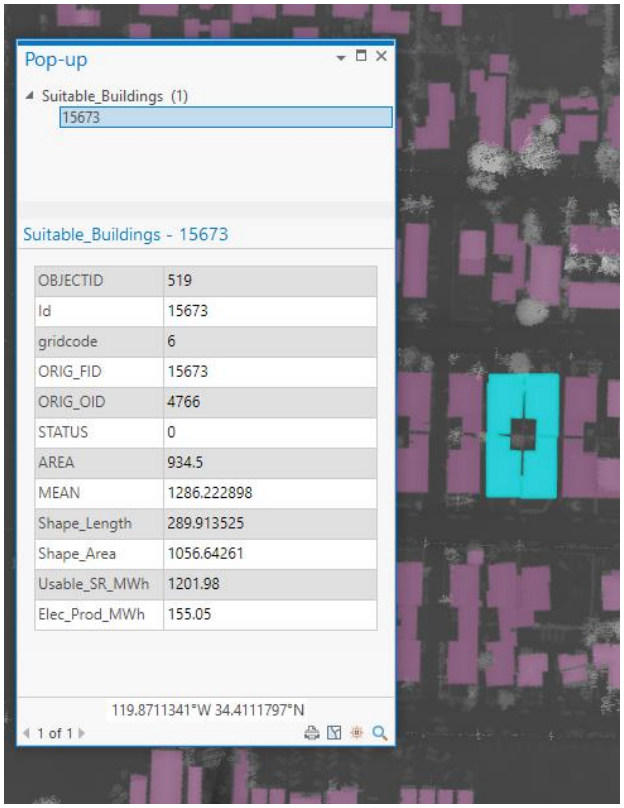

Figure 22: The statistics of one randomly selected building.

Based on the analysis, there is a total of 1.31 square kilometers of rooftop suitable for the solar PV installation, and the total possible annual electricity generation from rooftop solar PV can reach **208.67 GWh.** According to the U.S. Energy Information Administration, it requires 1.13 pounds of coal, or 0.08 gallons of petroleum liquids, or 7.43 cubic feet of natural gas to produce 1kWh of electricity on average(*U.S. Energy Information Administration (EIA)*, n.d.). This means if all the suitable roofs in the study area are covered with solar PV panels, $2.36 * 10^8$ pounds of coal, or equivalently $1.67 * 10^7$ gallons of petroleum liquids, or $1.55 * 10^9$ cubic feet of natural gas can be saved. Moreover, complete combustion of one pound of carbon can generate 3.667 pounds of carbon dioxide (Hong & Slatick, 1994). Assuming 78 percent of coal is carbon, the solar PV panels in the study area can prevent $2.94 * 10^6$ tons of carbon dioxide emission. Although complete combustion is impossible in real life, and the carbon concentration can vary depending on the location, this provides a rough estimation of how much CO2 can be reduced.

It is also important to understand the suitable areas for community solar. As it has been talked about in chapter 3, community solar has a wide range of definitions. Since this study only

covers roof areas and it is legitimate to consider multi-dwelling units, such as apartments, as potential sites for community solar programs, a subset of building footprints is made indicating the possible community solar sites, as shown in figure 23. This raster is made by filtering out any buildings with an area of less than 300 square meters. This is because according to (*Statista Research Department*, 2022), the average size of a single-family home built for sale in the United States amounted to 2,491 square feet, which equals 231.4 square meters. However, the polygons of two adjacent buildings might be connected when they are too close together. This will count two buildings as one large building, but in reality, they are not suitable for community solar programs. Since there is no systematic way to separate the buildings, a higher cut-off value, 300 square meters, is used to offset the extra areas misidentified as multi-dwelling units.

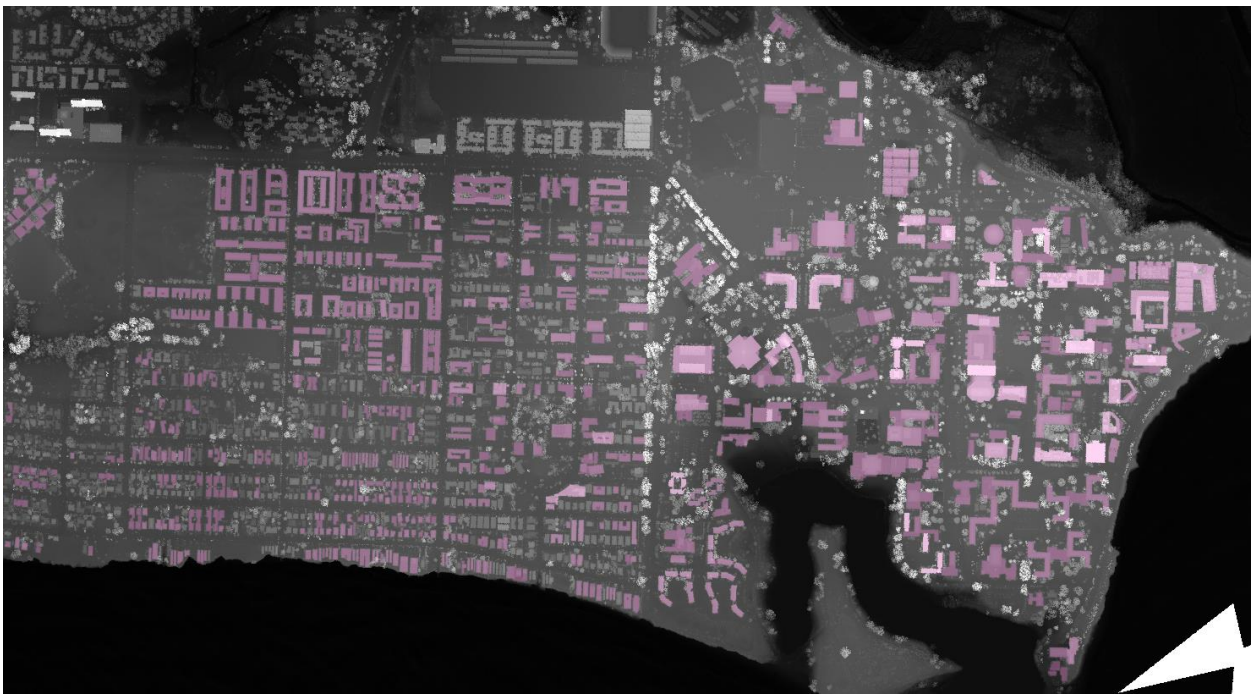

Figure 23: The building footprints of areas that are suitable for community solar programs.

The annual electricity generation from the possible community solar sites is **195.83MWh**, which accounts for 93.8 percent of the total annual generation. Two major reasons cause this extremely high proportion. Due to the proximity of Isla Vista to the UCSB campus,

there are many multi-dwelling units in Isla Vista to support a dense population. Besides, almost all buildings on the UCSB campus are considered suitable for community solar. Another factor is that the multi-dwelling units in the study area are often associated with flat roofs, while the single units often have sloped roofs. If the same calculation is applied to the solar community, $2.87 * 10^6$ pounds of carbon dioxide emission can be prevented.

According to the California Energy Commission, the annual electricity consumption in Santa Barbara County is 2763.4 GWh. If all suitable rooftops are covered with solar PV panels, about an extra 7.55% of electricity consumption can be offset by renewable energy for Santa Barbara County. However, the annual electricity from solar PV and solar thermal in 2020 in Santa Barbara County is only 93,242 MWh, which is a tiny part of the total electricity generation. As mentioned above, solar PV panels can play a vital role in achieving 100% renewable electricity in Santa Barbara, But compared to what we have now, there is still a long way to go.

Chapter 5: Conclusion

This project identifies and estimates the suitable areas for rooftop PV and solar PV potential in the Isla Vista and UCSB campuses. The study area, located in mid-latitude, receives abundant solar radiation throughout the year. Combined with the high population density in Isla Vista and the property of public use of the UCSB campus, the study area has great potential for community solar programs. The LiDAR data is used and processed in ArcGIS Pro to remove the unsuitable areas for PV installation and calculate the solar radiation.

Based on the analysis, there are a total of 1.31 square kilometers of rooftops suitable for the solar PV installation, and 93.84 percent (1.23 square kilometers) of those can support community solar. If all suitable areas are covered with solar PV panels with an average performance, the estimated annual electricity generation would be 208.67GWh, which can offset $2.94 * 10^6$ tons of carbon dioxide emission. If only the community solar program is considered, 195.83MWh of electricity can be produced annually. The result has shown that solar PV panels can play a significant role in the study areas to replace traditional fossil fuels. Even though the solar community program is hard to start, as mentioned above, UCSB, as an educational facility with stable funds and large energy consumption, has the ability to utilize the community solar program to the maximum extent. The existing solar program on the UCSB campus includes Campus Parking Structure II Solar Panels, Cheadle Hall Goes Solar, Parking Lot 38 Solar Panels, and Robertson Gym Rooftop Solar. Collectively, these solar panels are able to support 40 percent of campus energy demand at peak and provide approximately 15% of UCSB's annual electricity needs.

This study also provides implications for calculating the solar potential in rural/suburban areas with relatively high resolution and accuracy. There are many methods of calculating solar

potential, as mentioned in chapter 2, with each method designed for different study regions and scales. A systematic method with many assumptions is commonly used for large area calculation, and the parameters used for the city with high buildings are different from that for neighborhood units. Thus, this study provides a method specifically designed for small suburban areas with high building density but relatively low height. It is noticeable that since the average height of buildings is low, the method of differentiating the building from the surrounding is especially important in this study area and can be replicated somewhere else. Also, although the manual correction used in this study is not appropriate for large areas, it only serves as a way to improve accuracy. In other words, when the study area is broad, and the spatial resolution is relatively coarse, the accuracy level might not be needed as high as in this study and is often compensated for calculation time.

More research can be done on this topic. For example, one can calculate the cost of installing solar PV panels in the study areas and the payoff time. Also, this study does not consider the fact that some suitable areas are already covered with solar panels. Future research can compare the existing rooftop PV panels to the maximum potential capacity.

Admittedly, there are also some limitations of this study. Although the manual correction of building footprints works very well in this study due to the relatively small study area, it might not be applied to complex and large areas. A more sophisticated way, which finds a perfect balance between removing noise and keeping the necessary data, is required when calculating the solar potential in large areas. Also, even though the manual correction is good for smoothing the border and filling the holes, man-made mistakes could happen and might slightly affect the final results. Also, the aspect ranging from 300-to 60 is removed for the simplicity of calculation. However, if the method proposed by (Gergelova, Labant, et al., 2020) is strictly followed, the

calculation should take 292.5-67.5. This might also slightly change the final results. Moreover, when calculating the solar radiation, the calculation direction is reduced from 32 to 16 to reduce calculation time. More direction might lead to a more precise calculation. Lastly, this study's most noticeable deficiency is that the most suitable roof morphology for PV installation is not identified as proposed. This is because the reconstruction and categorization of the roof require the use of the 3D base map solution in ArcGIS Pro. To get access to these solutions, the ArcGIS Pro has to be at least version 2.8 or higher, but UCSB only provides a license for 2.7, and the new version will not be released until early July. However, this provides research topics for those interested in my thesis and who would like to continue the work.

References

Adeleke, A. K., & Smit, J. L. (2020). Building roof extraction as data for suitability analysis. *Applied Geomatics*, *12*(4), 455–466. https://doi.org/10.1007/s12518-020-00312-9

Aylett, A. (2013). Networked Urban Climate Governance: Neighborhood-Scale Residential Solar Energy Systems and the Example of Solarize Portland. *Environment and Planning C: Government and Policy*, *31*(5), 858–875. https://doi.org/10.1068/c11304

Bazán, J., Rieradevall, J., Gabarrell, X., & Vázquez-Rowe, I. (2018). Low-carbon electricity production through the implementation of photovoltaic panels in rooftops in urban environments: A case study for three cities in Peru. *Science of The Total Environment*, *622–623*, 1448–1462. https://doi.org/10.1016/j.scitotenv.2017.12.003

Brummer, V. (2018). Community energy – benefits and barriers: A comparative literature review of Community Energy in the UK, Germany and the USA, the benefits it provides for society and the barriers it faces. *Renewable and Sustainable Energy Reviews*, *94*, 187–196. https://doi.org/10.1016/j.rser.2018.06.013

Carneiro, C., Morello, E., & Desthieux, G. (2009). Assessment of Solar Irradiance on the Urban Fabric for the Production of Renewable Energy using LIDAR Data and Image Processing Techniques. In M. Sester, L. Bernard, & V. Paelke (Eds.), *Advances in GIScience* (pp. 83–112). Springer. https://doi.org/10.1007/978-3-642-00318-9_5

Clean Energy Future – Sustainability and Resilience – City of Santa Barbara. (n.d.). Retrieved May 12, 2022, from https://sustainability.santabarbaraca.gov/energy/

Community Solar Basics. (n.d.). Energy.Gov. Retrieved December 6, 2021, from https://www.energy.gov/eere/solar/community-solar-basics

Devabhaktuni, V., Alam, M., Shekara Sreenadh Reddy Depuru, S., Green, R. C., Nims, D., & Near, C. (2013). Solar energy: Trends and enabling technologies. *Renewable and Sustainable Energy Reviews*, *19*, 555–564. https://doi.org/10.1016/j.rser.2012.11.024

El Merabet, Y., Meurie, C., Ruichek, Y., Sbihi, A., & Touahni, R. (2015). Building Roof Segmentation from Aerial Images Using a Lineand Region-Based Watershed Segmentation Technique. *Sensors*, *15*(2), 3172–3203. https://doi.org/10.3390/s150203172

Electricity Consumption by County. (n.d.). Retrieved May 12, 2022, from https://ecdms.energy.ca.gov/elecbycounty.aspx

Electricity in the U.S. - U.S. Energy Information Administration (EIA). (n.d.). Retrieved November 6, 2021, from https://www.eia.gov/energyexplained/electricity/electricity-in-the-us.php

Flow Direction (Spatial Analyst)—ArcMap | Documentation. (n.d.). Retrieved December 4, 2021, from https://desktop.arcgis.com/en/arcmap/latest/tools/spatial-analyst-toolbox/flow-direction.htm

Frequently Asked Questions (FAQs)—U.S. Energy Information Administration (EIA). (n.d.). Retrieved April 11, 2022, from https://www.eia.gov/tools/faqs/faq.php

Gergelova, M. B., Kuzevicova, Z., Labant, S., Kuzevic, S., Bobikova, D., & Mizak, J. (2020). Roof's Potential and Suitability for PV Systems Based on LiDAR: A Case Study of Komárno, Slovakia. *Sustainability*, *12*(23), 10018. https://doi.org/10.3390/su122310018

Gergelova, M. B., Labant, S., Kuzevic, S., Kuzevicova, Z., & Pavolova, H. (2020). Identification of Roof Surfaces from LiDAR Cloud Points by GIS Tools: A Case Study of Lučenec, Slovakia. *Sustainability*, *12*(17), 6847. https://doi.org/10.3390/su12176847

Goetzberger, A., Hebling, C., & Schock, H.-W. (2003). Photovoltaic materials, history, status and outlook. *Materials Science and Engineering: R: Reports*, *40*(1), 1–46. https://doi.org/10.1016/S0927-796X(02)00092-X

Haala, N., Brenner, C., & Anders, K.-H. (1998). *3D URBAN GIS FROM LASER ALTIMETER AND 2D MAP DATA*. *XXXII*, 321–330.

Hernandez, R. R., Easter, S. B., Murphy-Mariscal, M. L., Maestre, F. T., Tavassoli, M., Allen, E.

B., Barrows, C. W., Belnap, J., Ochoa-Hueso, R., Ravi, S., & Allen, M. F. (2014). Environmental impacts of utility-scale solar energy. *Renewable and Sustainable Energy Reviews*, *29*, 766–779. https://doi.org/10.1016/j.rser.2013.08.041

Hetrick, W. A., Rich, P. M., Barnes, F. J., & Weiss, S. B. (1993). *GIS-based Solar Radiation Flux Models*. *3*, 132–143.

Hoffman, S. M., & High-Pippert, A. (2005). Community Energy: A Social Architecture for an Alternative Energy Future. *Bulletin of Science, Technology & Society*, *25*(5), 387–401. https://doi.org/10.1177/0270467605278880

Hoffman, S. M., & High-Pippert, A. (2010). From private lives to collective action: Recruitment and participation incentives for a community energy program. *Energy Policy*, *38*(12), 7567–7574. https://doi.org/10.1016/j.enpol.2009.06.054

Hong, B. D., & Slatick, E. R. (1994). Carbon dioxide emission factors for coal. *Quarterly Coal Report*. https://www.osti.gov/etdeweb/biblio/82283

Isla Vista, CA | *Data USA*. (n.d.). Retrieved November 22, 2021, from https://datausa.io/profile/geo/isla-vista-ca/

Isla Vista Food Cooperative | *RE-volv*. (n.d.). Retrieved January 16, 2022, from https://re-volv.org/project/islavistafoodcooperative/

Izquierdo, S., Rodrigues, M., & Fueyo, N. (2008). A method for estimating the geographical distribution of the available roof surface area for large-scale photovoltaic energy-potential evaluations. *Solar Energy*, *82*(10), 929–939. https://doi.org/10.1016/j.solener.2008.03.007

Kannan, N., & Vakeesan, D. (2016). Solar energy for future world: - A review. *Renewable and Sustainable Energy Reviews*, *62*, 1092–1105. https://doi.org/10.1016/j.rser.2016.05.022

Margolis, R., Gagnon, P., Melius, J., Phillips, C., & Elmore, R. (2017). *Using GIS-based methods and lidar data to estimate rooftop solar technical potential in US cities*. *12*(7), 074013. https://doi.org/10.1088/1748-9326/aa7225

Melius, J., Margolis, R., & Ong, S. (2013). *Estimating Rooftop Suitability for PV: A Review of Methods, Patents, and Validation Techniques* (NREL/TP--6A20-60593, 1117057; p. NREL/TP--6A20-60593, 1117057). https://doi.org/10.2172/1117057

Nguyen, H. T., & Pearce, J. M. (2012). Incorporating shading losses in solar photovoltaic potential assessment at the municipal scale. *Solar Energy*, *86*(5), 1245–1260. https://doi.org/10.1016/j.solener.2012.01.017

Nguyen, H. T., Pearce, J. M., Harrap, R., & Barber, G. (2012). The Application of LiDAR to Assessment of Rooftop Solar Photovoltaic Deployment Potential in a Municipal District Unit. *Sensors*, *12*(4), 4534–4558. https://doi.org/10.3390/s120404534

Parida, B., Iniyan, S., & Goic, R. (2011). A review of solar photovoltaic technologies. *Renewable and Sustainable Energy Reviews*, *15*(3), 1625–1636. https://doi.org/10.1016/j.rser.2010.11.032

Peters, M., Fudge, S., High-Pippert, A., Carragher, V., & Hoffman, S. M. (2018). Community solar initiatives in the United States of America: Comparisons with – and lessons for – the UK and other European countries. *Energy Policy*, *121*, 355–364. https://doi.org/10.1016/j.enpol.2018.06.022

Quirós, E., Pozo, M., & Ceballos, J. (2018). Solar potential of rooftops in Cáceres city, Spain. *Journal of Maps*, *14*(1), 44–51. https://doi.org/10.1080/17445647.2018.1456487

Razykov, T. M., Ferekides, C. S., Morel, D., Stefanakos, E., Ullal, H. S., & Upadhyaya, H. M. (2011). Solar photovoltaic electricity: Current status and future prospects. *Solar Energy*, *85*(8), 1580–1608. https://doi.org/10.1016/j.solener.2010.12.002

Sampaio, P. G. V., & González, M. O. A. (2017). Photovoltaic solar energy: Conceptual framework. *Renewable and Sustainable Energy Reviews*, *74*, 590–601. https://doi.org/10.1016/j.rser.2017.02.081

Seyfang, G., Park, J. J., & Smith, A. (2013). A thousand flowers blooming? An examination of community energy in the UK. *Energy Policy*, *61*, 977–989.

https://doi.org/10.1016/j.enpol.2013.06.030

Size of new single-family homes in the U.S. (n.d.). Retrieved April 11, 2022, from https://www.statista.com/statistics/529371/floor-area-size-new-single-family-homes-usa/

Solar Photovoltaic Technology Basics. (n.d.). Energy.Gov. Retrieved January 11, 2022, from https://www.energy.gov/eere/solar/solar-photovoltaic-technology-basics

Solar Rooftop Potential. (n.d.). Energy.Gov. Retrieved November 7, 2021, from https://www.energy.gov/eere/solar/solar-rooftop-potential

Solomon, S., Plattner, G.-K., Knutti, R., & Friedlingstein, P. (2009). Irreversible climate change due to carbon dioxide emissions. *Proceedings of the National Academy of Sciences*, *106*(6), 1704–1709. https://doi.org/10.1073/pnas.0812721106

Sovacool, B. K., & Lakshmi Ratan, P. (2012). Conceptualizing the acceptance of wind and solar electricity. *Renewable and Sustainable Energy Reviews*, *16*(7), 5268–5279. https://doi.org/10.1016/j.rser.2012.04.048

Subtil Lacerda, J., & van den Bergh, J. C. J. M. (2016). Diversity in solar photovoltaic energy: Implications for innovation and policy. *Renewable and Sustainable Energy Reviews*, *54*, 331–340. https://doi.org/10.1016/j.rser.2015.10.032

This Month in Physics History. (n.d.). Retrieved January 11, 2022, from http://www.aps.org/publications/apsnews/200904/physicshistory.cfm

Tian, J., & Xu, S. (2021). A morphology-based evaluation on block-scale solar potential for residential area in central China. *Solar Energy*, *221*, 332–347. https://doi.org/10.1016/j.solener.2021.02.049

US Department of Commerce, N. O. and A. A. (n.d.). *What is LIDAR*. Retrieved November 22, 2021, from https://oceanservice.noaa.gov/facts/lidar.html

US EPA, O. (2015, August 10). *Greenhouse Gases Equivalencies Calculator—Calculations and References* [Data and Tools]. https://www.epa.gov/energy/greenhouse-gases-equivalencies-calculator-calculations-and-references

Walker, G., & Devine-Wright, P. (2008). Community renewable energy: What should it mean? *Energy Policy*, *36*(2), 497–500. https://doi.org/10.1016/j.enpol.2007.10.019

Yimprayoon, C., & Navvab, M. (2010). *Quantification of available solar irradiation on rooftops using orthophotograph and LiDAR data*.